Models of the Bis-Histidine-Ligated Electron-Transferring Cytochromes. Comparative Geometric and Electronic Structure of Low-Spin Ferro- and Ferrihemes

ARTICLE *in* CHEMICAL REVIEWS · MARCH 2004

Impact Factor: 46.57 · DOI: 10.1021/cr020634j · Source: PubMed

1 AUTHOR:

F(rances) Ann Walker
The University of Arizona
240 PUBLICATIONS **8,648** CITATIONS

SEE PROFILE

Models of the Bis-Histidine-Ligated Electron-Transferring Cytochromes. Comparative Geometric and Electronic Structure of Low-Spin Ferro- and Ferrihemes

F. Ann Walker*

Department of Chemistry, University of Arizona, Tucson, Arizona 85721-0041

Received April 8, 2003

Contents

* E-mail: awalker@u.arizona.edu. Tel.: (520) 621-8645. Fax: (520) 626-9300.

1. Introduction

The word "cytochrome" was coined more than 100 years ago, in 1884 by McMunn, to describe the colored substances in cells.[1] Later, many of these "cytochromes" were found to contain hemes, that is to say, porphyrins complexed to iron.[2,3] The cytochromes *a*, *b*, *c*, *d*, *f*, and *o* are heme proteins that are involved in electron transfer; the iron cycles between Fe(III) and Fe(II) to allow the transfer of electrons from and to the redox cofactors of each of these cytochromes. The letter names in general are indicative of a common set of substituents on the periphery of the heme that give rise to particular optical spectral features when complexed to pyridine in their reduced (Fe(II)) state, sometimes called the "pyridine hemochrome" spectra. The names (heme *a*, *b*, *c*, *d*, d_1, *o*) are very old, and in some cases how they arose defies explanation. Only cytochromes *c* have the heme covalently attached to the protein, although in recent years a number of cases of modified hemes having unique types of covalent attachments to their proteins and unique spectral features have been reported. The heme of cytochrome *f* is a *c* heme—it is the axial ligands that give cytochrome *f* its particular spectroscopic features.

Another class of proteins that carries the name "cytochrome" is that of the enzymes called the cytochromes P450. These enzymes are monooxygenases that insert one atom of a dioxygen molecule into a substrate that is often, but not always, an organic molecule (including steroids, unsaturated hydrocarbons (to produce epoxides), xenobiotics, and a very

10.1021/cr020634j CCC: $48.50
Published on Web 01/07/2004

Ann Walker was born and raised in the small town of Adena, Ohio, near Wheeling, West Virginia, in the tri-state region of eastern Ohio, the West Virginia panhandle, and western Pennsylvania. At Adena High School, she was very active in music groups, including the marching and concert bands, clarinet quartet, and dance band. She obtained her B.A. degree in chemistry from The College of Wooster in 1962, and her Ph.D. in physical inorganic chemistry from Brown University in 1966, and she was then an NIH Postdoctoral Fellow with the late Daniel Kivelson at UCLA. Ann began her career as a chemistry professor at Ithaca College in 1967, and moved to San Francisco State University in 1970. She was recipient of an NIH Research Career Development Award for the period 1976–1981. In 1990, she moved to the University of Arizona, where she is currently Regents Professor in the Department of Chemistry, has a joint appointment in the Department of Biochemistry and Molecular Biophysics, and is a member of the Center for Insect Sciences. She teaches undergraduate and graduate courses in inorganic chemistry and magnetic resonance (both NMR and EPR spectroscopy). In 2000, she was recipient of the Francis P. Garvan/John M. Olin medal of the American Chemical Society. In 2001, she was recipient of the Luigi Sacconi medal of the Italian Chemical Society, and in late 2002, she received an Alexander von Humboldt Senior Research Fellowship in Science. With this fellowship she will spend part of her Sabbatical year (2003–2004) in the Physics Institute at the University of Lübeck, Germany. She will spend another part of her Sabbatical year at Stanford University, and the winter in Tucson. Ann is currently an Associate Editor of *J. Am. Chem. Soc*.

large number of other substrates), and produce one molecule of water with the other atom of dioxygen.[4] P450s also show activity as reductases, desaturases, dehalogenases, allene oxide synthases, prostacyclin and thromboxane synthases, etc. They are very numerous, with the genes for well over 1000 different enzymes having been identified.[5] Although these enzymes are so important that they comprise approximately 10% of the protein content of a healthy human liver, they are not the subject of this review, and they will thus not be considered further herein.

In any of the electron-transferring cytochromes, cytochromes *c* for example, the spectroscopic properties and reduction potentials of the individual members of the class are determined by a combination of a number of factors, including (i) the type of axial ligands bound to the heme, for example His-Met (as for mitochondrial cytochrome *c* and its bacterial counterparts), His-His (as for the cytochromes c_3 and a number of other multi-heme cytochromes), His-RNH_2 of the N-terminal amino group (as for cytochrome *f*), etc.; (ii) the orientation of axial ligands that have not only a σ-donor electron pair but also a π-donor orbital (usually filled) perpendicular to the σ-donor orbital (His, Met, Cys) that helps to determine the energy separation of the d_{xz}, d_{yz}, and d_{xy} orbitals of the low-spin Fe(III) center; (iii) the solvent accessibility of the heme; (iv) surface and buried charged groups near the heme and the charge type of the protein in which it is found, as well as the number of opposite charges present on its partner protein; (v) the dipoles of the protein backbone and side chains; (vi) changes in protein conformation and residue protonation; and (vii) solvent pH. The importance of (iii)−(vii) has recently been assessed,[6] while it has been difficult to evaluate and quantify the importance of (i) and (ii) (the subject of this review) in the absence of the others. Cytochromes are generally (except for the cytochromes c' [7−16]) six-coordinate and low spin in both the Fe(III) and Fe(II) states, so that in the process of electron transfer, only the oxidation state of the metal changes, thus minimizing the reorganization energy required to effect the electron transfer.

The cytochromes *b*, all of which contain heme *b* (also called protoheme or iron protoporphyrin IX), are found in the bc_1 complex of mitochondrial inner membranes of animals,[17−23] yeast,[24,25] bacteria,[26,27] algae, photosynthetic bacteria,[28−30] and the b_6f complex of chloroplasts,[17,31−33] as well as in liver microsomes,[34] outer mitochondrial membranes,[35] and erythrocytes,[36] and in certain enzymes such as sulfite oxidase,[37] sulfite,[38−40] nitrite[41−46] and nitrate[41−46] reductases, lactate dehydrogenase flavocytochrome b_2,[47,48] succinate:quinone oxidoreductase (SQR, also known as succinate dehydrogenase, and, for eukaryotes, as mitochondrial Complex II; however, not all of the SQR enzymes contain heme),[49] the related enzyme for the backward reaction, quinol:fumarate reductase (QFR, not all of which contain heme[50]),[51−53] and formate dehydrogenase-N.[54] A number of these cytochromes, including cytochrome b_5 (found in liver microsomes,[34] outer mitochondrial membranes,[35] and erythrocytes[36]), bacterial cytochromes bc_1[26] and c_3,[55−59] cytochromes bc_1 (b_{562} and b_{566}, or b_H and b_L),[17−32] chloroplast cytochrome b_6[32] and b_{559},[60−62] yeast flavocytochrome b_2,[47] the *b* heme of sulfite oxidase[37,63] heme-containing SQR,[49] heme-containing QFR,[51−53] formate dehydrogenase-N,[54] and four of the five *c* hemes of cytochrome *c* nitrite reductases,[44−46] have two histidines bound to the heme. Despite this common axial coordination, the reduction potentials of these proteins vary over a range of nearly 400 mV for the cytochromes *b*,[17−34,41,42,64,65] and an additional 300 mV for the cytochromes c_3.[55,66,67] To date, no comprehensive explanation of the reason(s) for this wide variation in reduction potentials has been achieved.

1.1. EPR Spectroscopic Data for Cytochromes: Identification of Axial Ligands and Their Orientations

Historically, EPR spectroscopy was used by Blumberg and Peisach[68,69] and others[70−73] to classify low-spin ferriheme proteins in terms of the axial ligands bound to the heme by analysis of the crystal field parameters ("tetragonality", Δ/λ, and "rhombicity", V/Δ) obtained from the three *g*-values of the rhombic spectra. The energy separation of the three formerly t_{2g} orbitals of strictly octahedral symmetry, split by the lower-symmetry field of the ferriheme center, in

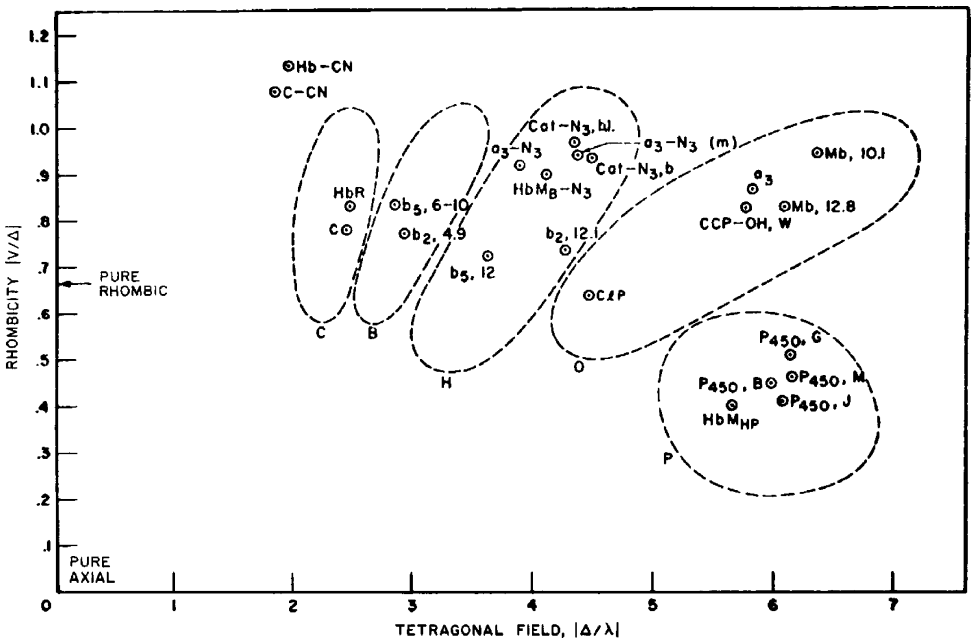

Figure 1. Crystal field parameters for ferric low-spin forms of various heme proteins: P450, J, P450, M, rabbit liver microsomal cytochrome P450; P450, B, rat liver microsomal P450; P450, G, bacterial cytochrome P450; HbM_{HP}, hemoglobin M(Hyde Park); ClP, chloroperoxidase; CCP−OH, W, cytochrome *c* peroxidase; Mb,12.8, sperm whale myoglobin, pH 12.8; Mb,10.1, sperm whale myoglobin, pH 10.1; a_3, cytochrome a_3; b_5, 12, cytochrome b_5, pH 12.1; b_2, cytochrome b_2, pH 12.1; HbM_B-N_3, hemoglobin M(Boston) azide; Cat-N_3,b, horse erythrocyte catalase azide; a_3-N_3(m), cytochrome a_3 azide, minority component; Cat-N_3, b.l, beef liver catalase azide; b_5, 4.9, cytochrome b_5, pH 4.9; b_5, 6−10, cytochrome b_5, pH 6−10; *c*, cytochrome *c*; HbR, hemoglobin(Riverdale); C-CN, cytochrome *c* cyanide; Hb-CN, ferrihemoglobin cyanide; ClP, chloroperoxidase. The analyses for ClP, C-CN, and Hb-CN are based on observation of two *g*-values and calculation of the third assuming $\sum g^2 = 16.0$, while all other points are based on three observed *g*-values. Original references to the spectral data provided in ref 68. Reprinted from ref 68. Copyright 1971 American Chemical Society.

units of the spin−orbit coupling constant λ, can be estimated from the following expressions:[70]

$$V/\lambda = E_{yz} - E_{xz} = g_{xx}/(g_{zz} + g_{yy}) + g_{yy}/(g_{zz} - g_{xx}) \quad (1)$$

$$\Delta/\lambda = E_{yz} - E_{xy} - {}^1/_2 V/\lambda = g_{xx}/(g_{zz} + g_{yy}) + g_{zz}/(g_{yy} - g_{xx}) - {}^1/_2 V/\lambda \quad (2)$$

The names given to the various "islands" of tetragonality and rhombicity values, P, O, H, B, and C,[68,69] shown in Figure 1, however, are indicative of the axial coordination of the heme of some well-known member of the class, rather than the particular substituents on the heme ring. This has led to some confusion among scientists who are unfamiliar with the vagaries of the historical names given. Molecular characterization of the heme centers that give rise to the P, O, H, B, and C tetragonalities and rhombicities showed each to have different axial ligation, with P-type centers having thiolate and a variety of possible sixth ligands, O-type centers having histidine and hydroxide ligation, H-type centers having two histidines with the imidazole rings of one or both deprotonated, B-type centers having two histidines with neutrally charged imidazole rings, and C-type centers having histidine−methionine coordination.[68,69]

More recently, single-feature low-spin ferriheme EPR signals with $g \geq 3.2$ have been observed for the cytochromes *b* of mitochondrial Complex III (ubiquinone:cytochrome *c* oxidoreductase) at very low temperatures (usually 10 K or lower),[71−78] as shown in Figure 2. These EPR signals could not be classified by the Blumberg−Peisach "Truth Diagrams"[68,69] because two of the three *g*-values were not resolved. Migita and Iwaizumi,[79] Carter, T'sai, and Palmer,[80] and we[81] showed that these single-feature,[74] "large g_{max}",[81] or highly anisotropic low-spin (HALS)[79] EPR signals could be generated by binding 2-methylimidazole (2-MeHIm) to Fe(III) proto-[79,80] or tetraphenylporphyrins.[81] Since then, we have shown that the model heme complex $[FeTPP(2\text{-}MeHIm)_2]^+$, which exhibits a "large g_{max}" EPR signal and magnetic Mössbauer spectrum with very large hyperfine splittings for a low-spin Fe(III) complex, arises from a molecular structure in which the axial ligands are *mutually perpendicular*.[82,83] We have recently called these Type I EPR and Mössbauer signals.[84,85] Strouse and co-workers[86] showed that the two unresolved *g*-values can be measured by single-crystal EPR spectroscopy at very low temperatures, and we have shown that they can be estimated by fits of the Mössbauer spectra recorded at 4.2 K in a large applied magnetic field.[82,85,87] The tetragonalities calculated using the *g*-values obtained in this manner are generally what would be expected for the axial ligation of the heme (P, O, H, B, C), but the rhombicities are much smaller, consistent with the fact that the d_{xz} and d_{yz} orbitals are of much more similar energy when the axial ligands are in perpendicular rather than parallel planes. It should be noted that there is a large difference in the apparent widths (in derivative mode) of the two *b* heme signals shown in Figure 2, with the b_{566} or b_L ($g = 3.75$) signal being

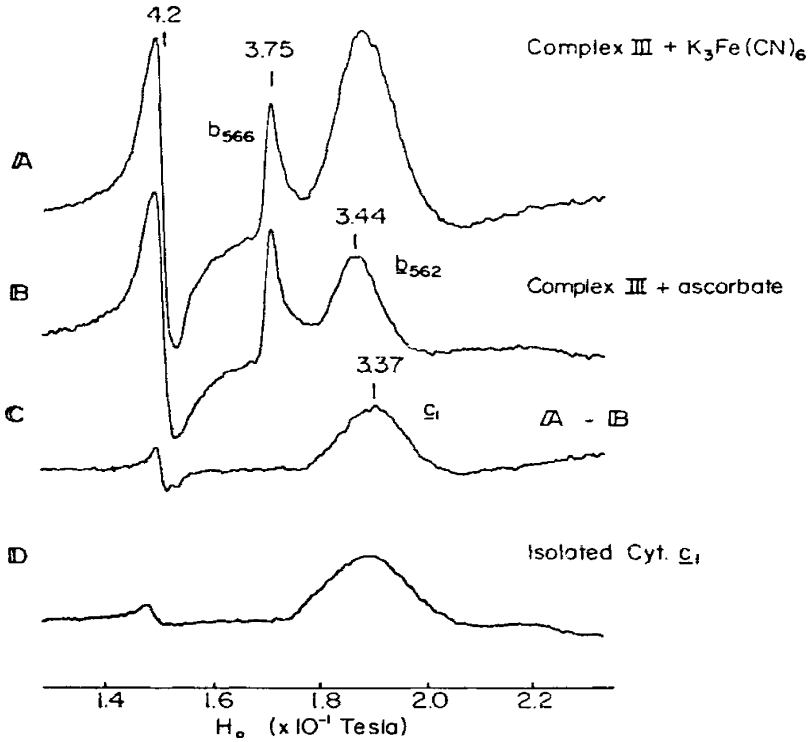

Figure 2. EPR spectra of Complex III recorded at 7 K. A, cytochromes b_{566} (b_H), b_{562} (b_L), and c_1 (fully oxidized by ferricyanide); B, cytochromes b_{566} (b_H) and b_{562} (b_L) (ascorbate reduced); C, cytochrome c_1 (A−B); D, isolated cytochrome c_1. Reprinted from ref 76. Copyright 1982 Academic Press/Elsevier.

much sharper than the b_{562} or b_H ($g = 3.44$) signal. Part of this difference in apparent widths is due to the inverse relationship between magnetic field and g-value (the latter of which is proportional to the energy of the electron spin transition), which crowds the $g = 3.75$ signal into fewer gauss than the $g = 3.44$ signal, but even so, the $g = 3.44$ signal is still comparatively broader, probably due to microheterogeneity of the b_{562} or b_H site, which thus gives rise to a range of possible g-values. Microheterogeneity is also one of the major reasons, along with g-strain, that the other two g-values of "large g_{max}" signals are not observed.[77]

The b cytochromes of mitochondrial Complexes II and III and cytochrome b_6 of plants each have two hemes that have bis-histidine coordination, with the ligands assumed to be in perpendicular planes (based on the "large g_{max}" EPR signals observed[74−78]). For bovine heart mitochondrial Complex III,[22] for which the resolution of the structure is now 2.2 Å,[88] it appears that heme b_L has an 83° histidine imidazole plane dihedral angle with individual imidazole planes of $\varphi_1 = 36°$ and $\varphi_2 = -47°$ to the $N_{II}-N_{IV}$ (N_C-N_A crystallographic) axis of the heme, $\Delta\varphi = 83°$, as defined in Figure 3. In contrast, heme b_H appears to have an imidazole plane dihedral angle $\Delta\varphi$ of 38°, with individual imidazole plane orientations of $\varphi_1 = -9°$ and $\varphi_2 = 29°$ to the same axis of this heme.[88] The histidine imidazole planes of heme b_H appear to bind off-axis (tilted from the heme normal) as well, and it has been suggested that such off-axis tilting of the axial ligands may be one reason for the "large g_{max}" signal;[89] this possibility will be considered further at the end of this review. Based on the results of recent studies of the structures and EPR spectra of model heme complexes to be discussed below, it is possible that this may be too small a dihedral angle for the observed[75] "large g_{max}" EPR signal. However, the minimum dihedral angle that gives rise to this type of EPR signal is not yet known; the work summarized in this review has narrowed that minimum angle to $70° \geq \Delta\varphi \geq 30°$.

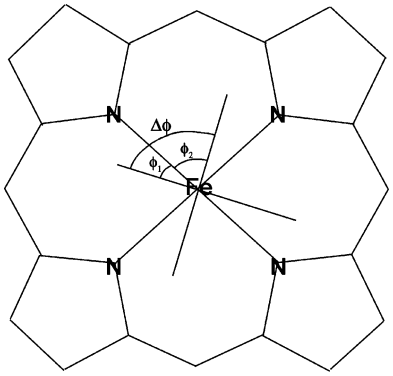

Figure 3. Diagram of the porphyrin core with two planar axial ligands shown as lines. The angles φ_1, φ_2, and $\Delta\varphi$ are defined. If the angle $\Delta\varphi$ is either 0 or 90°, then only one angle, φ, is given. Although the pyrroles of the hemes of the cytochromes and various other heme proteins have a customary numbering scheme (A−D) in X-ray crystallographic structure determinations, the definition of φ in this section does not depend on that scheme.

1.2. Reduction Potentials of Cytochromes, and Correlation with EPR *g*-Values

Among the systems known to have two histidines bound to the heme, probably in "perpendicular" planes (based upon the "large g_{max}" EPR signals observed), the cytochromes b of mitochondrial complexes II and III generally have at least one reduction

Table 1. EPR and Electrochemical Data for Cytochromes *b* from Mitochondrial Complexes II and III and Related Systems

organism, system, conditions	heme b_H		heme b_L		ref
	g_{max}	E_m, mV (pH)	g_{max}	E_m, mV (pH)	
B. subtilis Complex II					
membrane-bound	3.68	+16 (7.4)	3.42	−132 (7.4)	90, 91
purified complex		+65 (7.4)		−95 (7.4)	90
bovine heart Complex III					
membrane-bound	3.41	+105 (7.0)	3.75	−5 (7.0)	75, 92
	3.44	+92 (7.0)	3.71, 3.79	−31 (7.0)	75, 93
purified cyt. *b*		−5 (7.0)		−85 (7.0)	92
purified complex		+93 (7.2)		−34 (7.2)	95
complexed with *Rh. sphaeroides* reaction center		+80 (7.0)		−60 (7.0)	94
pigeon heart Complex III		+60 (7.2)		−25 (7.2)	96
		+40 (7.0)		−30 (7.0)	
yeast Complex III					
membrane-bound, deoxycholate buffer	3.60	+62 (7.4)	3.76	−20 (7.4)	24
taurocholate buffer		+98 (7.4)		+40 (7.4)	24
purified cyt. *b*	3.70	−44 (7.0)	3.70	−44 (7.0)	98
SDS-treated			2.90		98
A. aeolicus cytochrome bc_1	3.45	−60 (7.0)	3.7	−190 (7.0)	27
spinach chloroplast cyt. b_6f from PSI					
purified membranes	~3.7	+70 (7.0)	~3.7	−50 (7.0)	32
	3.60	−45 (7.0)[a]	3.60	−150 (7.0)	99, 100
spinach chloroplast cyt. b_{559} from PSII					
purified membranes[b]	3.08, 2.15[c]	+375 (6.5) (44%)		+228 (6.5) (31%)	64
				+57 (6.5) (25%)	
with 17- and 23-kDa extrinsic proteins removed[b]	3.04, 2.17[c]	+375 (6.5) (18%)		+171 (6.5) (42%)	64
				+3 (6.5) (40%)	
T. elongatus b_{559}					
intact PSII core[d]	3.08, 2.16[c]	+390 (6.5) (50%)		+275 (6.5) (50%)	65

[a] A third *b* heme was found having an absorbance peak at 560 nm and a midpoint potential of +47 mV.[99] [b] Three potentials observed for the single heme of this protein.[64] [c] Two *g*-values resolved.[64,65] [d] Two potentials observed for the single heme of this protein.[65]

potential that is much more positive than those for which the axial ligand planes are known to be mutually parallel. Specific reported reduction potentials and EPR *g*-values for complexes II and III from various species are listed in Table 1. For *Bacillus subtilis* succinate:quinone oxidoreductase (Complex II), the two *b* hemes have different reduction potentials, with b_H $E_{m'} = +16$ mV and $g_{max} = 3.68$, while b_L has $E_{m'} = -132$ mV and $g_{max} = 3.42$;[90,91] in the purified complex the reduction potentials of the two hemes are somewhat more positive.[90] In the case of bovine heart mitochondrial b_{566} and b_{562}, or b_H and b_L (Complex III), the "large g_{max}" signals of the native form of this complex occur at *g*-values of 3.41−3.44 and 3.75−3.78,[24,74] and the reduction potentials are reported to be +105 to +60 and −5 to −34 mV,[24,92−97] respectively, depending upon pH, the nature of the buffers used, methods of sample preparation, redox state of other redox centers present, presence or absence of the quinone, and possibly also upon the concentration of dyes used to measure the potentials.[98] Likewise, for the cytochrome bc_1 complex of the very different organism, the naphthoquinol-oxidizing hyperthomophilic bacterium *Aquifex aeolicus*, the g_{max}-values of b_H and b_L are 3.45 and 3.7, but the reduction potentials are much lower, −60 and −190 mV, respectively. Note that the high-potential heme has the larger *g*-value in Complex II, while the low-potential heme has the larger *g*-value in Complex III, and chloroplast cytochrome b_6f of photosystem I has *b* hemes with potentials that differ by more than 100 mV yet the *g*-values of the two are identical; it thus appears that there may be no correlation between the *g*-value of these "large g_{max}" features and the reduction potential of the heme.

Upon isolation of the mitochondrial Complex III cytochrome *b* protein from the complex, the potentials drop to −5 and −85 mV (bovine heart)[92] and −44 mV (both hemes) (yeast).[98] The EPR signal for both hemes of the latter species is found at $g_{max} = 3.70$, but upon treatment of the isolated cytochrome *b* with SDS denaturing buffer the EPR signal changes to the normal rhombic type, with $g = 2.9$.[98] In the case of spinach chloroplast cytochrome b_6 from Photosystem I, the two *b* hemes were reported to have reduction potentials of +70 and −50 mV,[32] but more recent work indicates that there are actually three types of *b* heme present, having midpoint potentials of +47, −45, and −150 mV at pH 7.0.[99] Upon denaturation of this protein in Triton X-100, the "large g_{max}" signals move from $g = \sim 3.7$ (later measured more accurately as 3.60[100]) to $g = 2.9$,[32] suggesting that the planes of the axial ligands have "relaxed"[71] to the parallel orientation. Cytochrome b_{559}, a mono-heme protein that is part of Photosystem II and is composed of two polypeptides (4 and 9 kDa), each of which contributes one histidine, appears to exist in three forms, high potential ($E_m = 375$ mV), intermediate potential ($E_m = 228$ mV), and low potential ($E_m = 57$ mV) at pH 6.5; removal of two extrinsic proteins thought to shield the heme center of b_{559} shifts the potentials to 375 (18%), 171 (42%), and 3 mV (40%) at the same pH.[64] The reasons for the observation of multiple reduction potentials are not known at present, although it is likely that the specific treatment of the large protein complex may alter this center in some

of the molecules. The EPR spectra, although broad, show two resolved features at $g = 3.08$, 2.15 and 3.04, 2.17, respectively;[64] thus, these are actually rhombic EPR signals similar to those of cytochromes *c*, in which the third *g*-value is not resolved but should be about 1.4. The reason for the observation of two EPR signals is not currently known. For the cyanobacterium *Thermosynechococcus elongatus*, cytochrome b_{559} has two reduction potentials at pH 6.5, +390 and +275 mV, and all three *g*-values are resolved (3.08, 2.16, and 1.41, leading to typical B (Figure 1) heme crystal field parameters, $\Delta/\lambda = 3.60$ and $V/\Delta = 0.43$).[65] Hence, these are not "large g_{max}" centers. Nevertheless, the high values of the reduction potentials are striking, and the data for this protein are thus included in Table 1.

In comparison, the water-soluble microsomal cytochromes b_5, which are bound to histidines in nearly parallel planes and have rhombic EPR spectra with *g*-values of 3.03, 2.23, and 1.4,[101] have reduction potentials near 0 mV vs NHE.[102−105] One exception to this is the outer mitochondrial membrane (OMM) cytochrome b_5, which, although it has the same EPR *g*-values, has a reduction potential of −102 mV,[106] even though it has seemingly conservative amino acid replacements almost identical optical, EPR, and NMR spectra[107] and structure,[108] as compared to the microsomal cytochromes b_5.

There has been only one water-soluble mono-heme cytochrome reported thus far that is bis-histidine-coordinated and gives a "large g_{max}" EPR signal ($g = 3.65$)[108] in the oxidized state. This is the bacterial cytochrome *c* from *Methylophilus methylotrophus*, and it loses one histidine ligand in its pH-linked reduction to the Fe(II) state.[109−111] However, in the membrane-bound cytochromes, such as the *b* heme centers of Complexes II and III, which exhibit "large g_{max}" EPR signals in their native states,[74−78,90−100] there is no pH-linked loss of an axial ligand upon reduction. Additionally, most of the cytochromes c_3 (also bis-histidine-coordinated) have one heme that gives a "large g_{max}" EPR signal,[66,67] and the identity of this heme can be determined from the structure, where one heme has a large dihedral angle $\Delta\varphi$ between the histidine imidazole planes.[56] Likewise, the reduction potential of this heme can be determined by the disappearance of the unique "large g_{max}" signal when this heme becomes reduced.[67] As in the cases of the membrane-bound cytochromes, for the cytochromes c_3 there is no pH-linked loss of an axial ligand upon reduction.[67] The pH-linked loss of a histidine ligand by cytochrome *c* upon reduction,[109−111] as well as the change in reduction potential and "relaxation" of the EPR signals of the membrane-bound cytochromes to the normal rhombic type upon removal of the protein from the natural membrane environment, both suggest that the existence of perpendicular axial ligand planes represents a higher energy ligand binding mode than having the axial ligands in parallel planes. The possible reasons for this have been sought through investigations of the structures, EPR and Mössbauer spectra, and the reduction potentials of a number of different types of model heme complexes, to be discussed below. The preparation and investigation of such model heme complexes is the subject of the remainder of this review. A chronological treatment is presented, because our understanding of the important factors that determine the structure of these complexes, and if and how the structures relate to their spectroscopic and redox properties, has developed stepwise as different systems have been investigated and new information has thus been obtained.

2. Iron Tetraphenylporphyrinates: The Early Complexes and Findings

As mentioned above, it was shown in the early 1980s that "large g_{max}" or HALS EPR signals could be obtained upon binding 2-methylimidazole to either Fe(III) protoporphyrin IX or Fe(III) tetraphenylporphyrins.[79−81] The structure of the $[TPPFe(2\text{-}MeHIm)_2]^+ClO_4^-$ complex, although known and often cited as an abstract from an American Chemical Society meeting in 1978,[112] probably one of the most cited ACS abstracts in history, was finally published in 1987.[83] It showed that the imidazole ligands are aligned at angles $\varphi_1 = -58°$ and $\varphi_2 = 32°$ to the nearest N_P-Fe-N_P axis, with a dihedral angle between the two imidazole ligands $\Delta\varphi = 89°$ (see Figure 3 for angle definitions), and that the porphyrinate ring is severely ruffled, with the *meso*-carbons alternating above and below the mean plane of the porphyrin ring by $|\Delta C_m| = 0.39$ Å.[83] The details of this structure will be discussed after we consider the structures of non-hindered imidazole complexes having ligands in parallel planes.

2.1. Non-Hindered Bis-Imidazole Complexes of TPPFe(III)

In a companion paper to that describing the structure of $[TPPFe(2\text{-}MeHIm)_2]^+ClO_4^-$,[83] the second report of the structure of the non-hindered bis-imidazole complex, $[TPPFe(HIm)_2]^+Cl^-$, was presented.[113] (The first reported structure[114] will be discussed below.) In the second structure,[113] the unit cell contains two molecules, each of which has the imidazole ligands in perfectly parallel planes, as required by the crystal symmetry. In one molecule the angle φ between the closest N_P-Fe-N_P axis and the projection of the ligand planes is 6°, while in the other this angle is 41°; interestingly, in the molecule with small φ, the $Fe-N_P$ bond lengths of the nearly eclipsed N_P-Fe-N_P are greater than those that are nearly perpendicular to the imidazole ligand planes (2.002 and 1.985 Å, respectively; average 1.994 Å) and the axial ligand $Fe-N_{ax}$ bonds are longer (1.977 Å), while for the molecule with large φ, the difference in bond lengths is much smaller (1.995 and 1.990 Å, respectively, average 1.993 Å) and the $Fe-N_{ax}$ bonds are shorter (1.964 Å).[113] Hence, the structure of the molecule with small φ appears to show a Jahn−Teller distortion[115] that would be consistent with the half-filled d_π orbital being oriented perpendicular to the imidazole ligand plane, where it could best interact with the filled p_π orbital on the bonding nitrogen of the imidazole ring of each ligand by $L\rightarrow Fe$ π donation to that half-filled d_π orbital (although charge-iterative

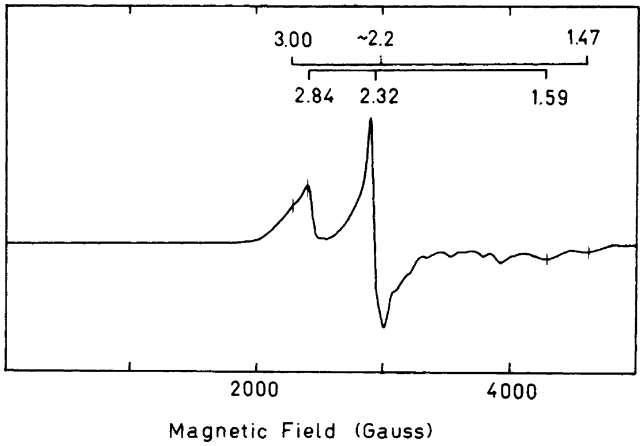

Figure 4. EPR spectrum of a small number of crystallites of $[TPPFe(HIm)_2]^+Cl^-$. Because of the small number of crystallites, a true powder EPR spectral shape was not achieved, as evidenced by the additional bumps between 3200 and 4100 G. The relevant *g*-values of the two species are grouped above the spectrum on the basis of $\sum g^2 = 16.0$. Reprinted from ref 82. Copyright 1986 American Chemical Society.

extended Hückel calculations had earlier suggested that the metal's empty $4p_\pi$ orbital might be more important in determining the orientation of the axial ligand[116]). Much later, this same idea was developed to explain the contact and pseudocontact shifts of ferriheme proteins, based upon the orientation of the axial histidine imidazole plane or the methionine thioether-filled p_π orbital nodal plane,[117] or the average of the two if both ligands contribute equally.

An understanding of the orbital energies involved in these two bis-imidazole ligand complexes of TPPFe(III) was obtained from a detailed EPR and Mössbauer spectroscopic study[82] that was actually carried out and published before the structures appeared. In this study it was shown that for polycrystalline samples of $[TPPFe(HIm)_2]Cl$, for which there were two molecules in the unit cell,[113] two overlapping EPR signals were observed with different *g*-values, rhombicities, and tetragonalities (Figure 4, Table 2). We suggested that the signal with smaller tetragonality and larger rhombicity arose from the molecules with small angle φ (which showed a structural Jahn−Teller distortion and had longer $Fe-N_{ax}$ bonds[113]), while the signal with larger tetragonality and smaller rhombicity arose from those having large angle φ (and shorter $Fe-N_{ax}$ bonds[113]).[82] Strouse and co-workers later investigated this crystalline complex by single-crystal EPR spectroscopy and verified that this was the case.[118] Detailed analysis of the structures and single-crystal EPR spectra of several (parallel) bis-imidazole ligand complexes of TPPFe(III) led to a quantitative relationship between the angle φ and the rhombicity,

Table 2. EPR *g*-values, Crystal Field Parameters, and Mössbauer Quadrupole Splittings for Key Model Heme Complexes

complex	$\Delta\varphi$, deg	$\sum$ off-axis tilts, deg[a]	g_1	g_2	g_3	$\sum g^2$	V/λ	Δ/λ	V/Δ	ΔE_Q, mm/s	ref
				Type II Complexes							
$[TPPFe(HIm)_2]^+$											
molecule 1	0		1.47	~2.2	3.00	16.00	1.73	3.53	0.49		82
molecule 2	0		1.59	2.32	2.84	15.98	2.15	3.12	0.69		82
$[TPPFe(HIm)_2]Cl$										2.23	172
$[OEPFe(4\text{-}NMe_2Py)_2]^+$	0		1.63	2.28	2.82	15.80	2.24	3.54	0.63	2.15	87
$[TPPFe(4\text{-}MeIm)_2]^-$	18		1.82	2.24	2.60	15.09	3.25	4.94	0.66		120
paral-$[TMPFe(5\text{-}MeHIm)_2]^+$	26, 30	5.7, 10.2	1.66	2.38	2.72	15.82	2.57	2.81	0.91	2.56	135
paral-$[OMTPPFe(1\text{-}MeIm)_2]^+$	19.5	7.5	1.54	2.51	2.71	16.02	2.44	1.82	1.34	2.80	163
paral-$[OMTPPFe(1\text{-}MeIm)_2]^+$ [b]			1.59	2.32	2.83	15.92	2.18	3.10	0.70		163
paral-$[OETPPFe(1\text{-}MeIm)_2]^+$ [c]			1.62	2.36	2.75	15.76	2.41	2.82	0.85		163
paral-$[OETPPFe(1\text{-}MeIm)_2]^+$ [b]			1.66	2.38	2.72	15.76	2.41	2.82	0.85		162
paral-$[TC_6TPPFe(1\text{-}MeIm)_2]^+$			1.43	2.41	2.84	15.92	1.98	2.23	0.89		163
paral-$[TC_6TPPFe(1\text{-}MeIm)_2]^+$ [b]			(1.45)[d]	2.39	2.86	16.00	1.97	2.33	0.85		163
				Type I Complexes							
$[TPPFe(2\text{-}MeHIm)_2]^+$	89	14.9	0.85[e]	1.93[e]	3.41	16.00	0.92	2.88	0.32	1.71	82
$[TMPFe(4\text{-}NMe_2Py)_2]^+$	79	9.6	0.92[e]	1.80[d]	3.44	15.92	0.89	3.20	0.28	1.75	87
$[TMPFe(1,2\text{-}Me_2Im)_2]^+$	90				3.17[f]					1.25	140
perp-$[TMPFe(5\text{-}MeHIm)_2]^+$	76	20.1			3.12					1.78	135
perp-$[OMTPPFe(1\text{-}MeIm)_2]^+$	90	0	0.63[e]	1.53[e]	3.61	15.77	0.67	3.93	0.17	1.76	163
perp-$[OMTPPFe(1\text{-}MeIm)_2]^+$ [b]					3.12						163
perp-$[OETPPFe(1\text{-}MeIm)_2]^+$	73.1	5.8	1.14[e]	2.00[e]	3.27	15.99	1.16	3.44	0.34	1.94	163
perp-$[OETPPFe(1\text{-}MeIm)_2]^+$ [b,c]					3.12						162
$[OETPPFe(4\text{-}NMe_2Py)_2]^+$	70	8.6			3.29						162
$[OETPPFe(4\text{-}NMe_2Py)_2]^+$	70		0.99[e]	1.95[e]	3.35					1.89	163
$[OETPPFe(4\text{-}NMe_2Py)_2]^+$ [b]	70				3.27						163
$[TC_6TPPFe(1\text{-}MeIm)_2]^+$	90	0			3.64						163
$[TC_6TPPFe(1\text{-}MeIm)_2]^+$ [b]					3.14						163
A:$[OMTPPFe(4\text{-}NMe_2Py)_2]^+$	79	0									163
B:$[OMTPPFe(4\text{-}NMe_2Py)_2]^+$	89	4.9									163
$[OMTPPFe(4\text{-}NMe_2Py)_2]^+$ [b]					3.29						163
C:$[OMTPPFe(2\text{-}MeHIm)_2]^+$	82	14									163
D:$[OMTPPFe(2\text{-}MeHIm)_2]^+$	81	4									163
$[OMTPPFe(2\text{-}MeHIm)_2]^+$ [b]					3.27						163

[a] Sum of the deviations of the planes of the axial ligands from the heme normal, in degrees. [b] Frozen solution. [c] Decomposed crystals. [d] Calculated from $\sum g^2 = 16$. [e] *g*-values determined from magnetic Mössbauer spectroscopy.[82,87,166] [f] For 2-MeHIm.[131]

V/Δ.[119] Hence, in a well-characterized system it may be possible to assign EPR signals on the basis of logical structural arguments.

The structure, spectroscopy, and electrochemistry of the bis-(imidazolate) complex, [K(K222)][TPPFe-(4-MeIm)$_2$], was reported by Quinn, Strouse, and Valentine in 1983.[120] This molecule has the two axial ligands with angles φ_1 and φ_2 from the nearest N_P-Fe-N_P axis of $-1°$ and 17°, yielding a dihedral angle between the two ligand planes, $\Delta\varphi = 18°$. Likewise, the two ligands have different $Fe-N_{ax}$ bond lengths, 1.928(12) Å for the ligand having $\varphi_2 = 17°$ and 1.958-(12) Å for the ligand having $\varphi_1 = -1°$.[120] Although not a statistically significant difference, it is interesting to note that the longer $Fe-N_{ax}$ bond length does correlate with the smaller angle φ. Compared to the second structure of [TPPFe(HIm)$_2$]Cl,[113] these $Fe-N_{ax}$ distances are shorter by as much as 0.05 Å, and up to 0.06 Å shorter than the longest $Fe-N_{ax}$ distance of the first structure of [TPPFe(HIm)$_2$]Cl,[114] to be discussed below. Hence, it is not surprising that the tetragonality calculated for the [TPPFe(4-MeIm)$_2$]$^-$ complex is larger ($\Delta/\lambda = 4.94$)[120] than for the two molecules of [TPPFe(ImH)$_2$]$^+$ ($\Delta/\lambda = 3.53, 3.12$),[82] since tetragonality is a measure of ligand field strength[68−70] and we would expect imidazolate to be a stronger-field ligand than neutral imidazole. The $Fe-N_P$ bond distances alternate, with two trans bonds being somewhat longer than the other two (2.031(12), 2.006(12) Å vs 1.974(11), 1.982(11) Å),[120] possibly suggesting the same type of Jahn−Teller distortion as observed in the $\varphi = 6°$ molecule of [TPPFe(HIm)$_2$]Cl.[113]

2.2. Hindered Bis-Imidazole Complexes of TPPFe(III)

For the bis-2-methylimidazole complex, [TPPFe(2-MeHIm)$_2$]$^+$ClO$_4^-$, with perpendicular ($\Delta\varphi = 89°$) axial ligand planes,[83] the EPR spectrum at 13 K or lower exhibited mainly a "large g_{max}" signal with $g = 3.41$,[82] Figure 5. (A high-spin Fe(III) EPR signal is also typically observed in polycrystalline samples because of loss of a ligand from molecules on the surface of the crystallites, and this signal can appear very intense in the derivative-mode spectra, because it is not broadened as much by electron spin−spin relaxation as are the signals of the bulk sample. This sensitivity to surface molecules means that EPR spectra of crystalline solid samples have distorted signal intensities that favor the spectra of the surface molecules. In comparison, Mössbauer spectroscopy senses all of the iron present.) The "large g_{max}" signal was obtained both for the crystallites and for frozen dimethylformamide solutions of the complex, as shown in Figure 5, suggesting that the structure of the complex in frozen solution is the same as that in the solid state. (Later ^{1}H NMR studies of the TMPFe-(III) analogue of this complex showed that the number of *ortho*-methyl and pyrrole-H resonances observed and the chemical exchange cross-peaks observed in the NOESY/EXSY spectra are consistent with the axial 2-MeHIm ligands being in perpendicular planes over the *meso*-carbons in homogeneous solution at ambient temperatures,[121,122] as observed in the crystalline state.[83]) Magnetic Mössbauer spectra of these samples allowed estimation of the other two EPR g-values: If the sum of the squares of the g-values, $\sum g^2 = g_1^2 + g_2^2 + g_3^2$, is taken to be 16.0, then the values of g_2 and g_1 are 1.93 and 0.85, respectively, leading to a tetragonality of 2.88 and rhombicity of 0.32,[82] Table 2; the much smaller value of the rhombicity is consistent with more-nearly degenerate d_π orbitals, d_{xz} and d_{yz}, for this complex than for those having their axial ligands in parallel planes.[82]

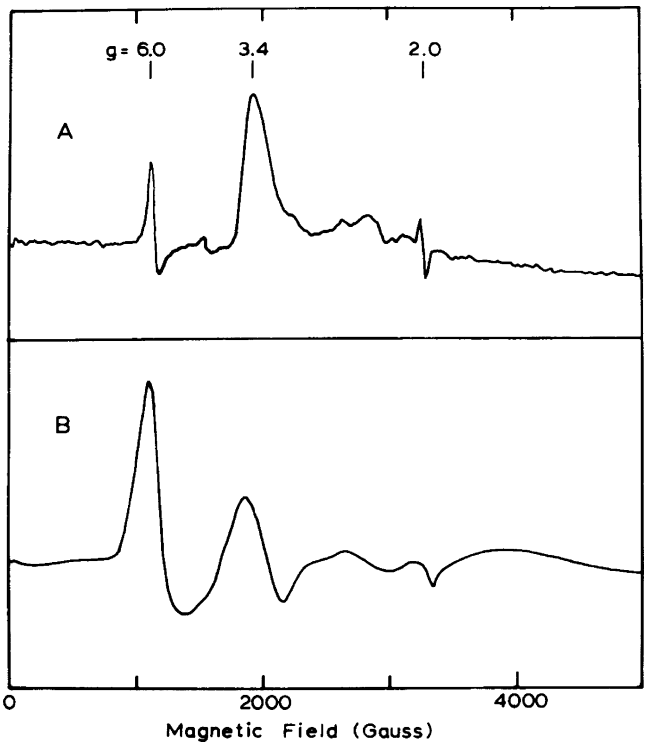

Figure 5. EPR spectra of [TPPFe(2-MeHIm)$_2$]$^+$Cl$^-$: (A) DMF glass; (B) crystalline form. The Fe(III) concentration in DMF was 5 mM, and the sample was 94% enriched in ^{57}Fe. The crystals were not enriched in ^{57}Fe. They were suspended in mineral oil. The high-spin Fe(III) impurity signal at $g = 6.0$ is due to about 15% of the iron present, but appears as an intense signal due to the much greater transition probability for this high-spin species than for the low-spin "large g_{max}" species whose signal appears at $g = 3.4$. Reprinted from ref 82. Copyright 1986 American Chemical Society.

Another interesting finding in that EPR/Mössbauer study[82] was that crystals of the 2-methylimidazole complex of OEPFe(III) exhibited a high-spin EPR signal and had previously been shown by X-ray crystallography to have the axial ligands in parallel planes with much longer $Fe-N_{ax}$ bonds and a magnetic moment consistent with a high-spin Fe(III) complex,[123] while the same complex dissolved and frozen in methylene chloride yielded a "large g_{max}" EPR signal ($g = 3.56$) indicative of a low-spin Fe(III) complex.[82] The low-spin complex has not been crystallized; it is not stable in the low-spin state at room temperature.[123]

In that EPR/Mössbauer work we also suggested[82] that the crystal field parameters obtained from the three g-values[68,70] can allow estimation of the difference in reduction potential between heme centers in

which axial ligands are held in parallel as compared to perpendicular planes. However, this idea was based upon there being no difference in energy for parallel and perpendicular orientations of axial ligands for the Fe(II) states of these heme centers, which is now known not to be the case: The vast majority of Fe(II) porphyrinates have their axial ligands in parallel planes,[124,125] and as will be discussed in detail below, there appears to be a perhaps surprisingly strong preference for this axial ligand plane orientation for Fe(II) porphyrinates.

2.3. The Enigmatic Bis-Imidazole Complex of TPPFe(III) with Large Axial Ligand Plane Dihedral Angle

The first reported structure of $[TPPFe(HIm)_2]^+$ was that of $[TPPFe(HIm)_2]^+Cl^-\cdot CH_3OH$, the work of Collins, Countryman and Hoard.[114] This was not only the first structure of this molecule, but actually the first structure of a low-spin Fe(III) porphyrinate to be reported in the literature. Unlike the second structure of this complex,[113] the first structure did not have the imidazole ligands in parallel planes, but rather had a dihedral angle $\Delta\varphi = 57°$, with the individual imidazoles having $\varphi_1 = -18°$ and $\varphi_2 = 39°$ from one N_P-Fe-N_P axis. The two ligands had different $Fe-N_{ax}$ bond lengths, 1.957(4) and 1.991(5) Å, respectively, and the porphyrin core was ruffled ($|\Delta C_m| = 0.305$ Å); the $Fe-N_P$ bond lengths (1.989 Å) were thus shorter than those for a flat porphyrinate ring.[114] With the large dihedral angle between axial ligand planes, it is unfortunate that the EPR spectrum of this complex was not recorded, to determine whether it had a normal rhombic or a "large g_{max}" type of signal. But this structure was solved nearly 10 years before the first "large g_{max}" signals were observed for model heme complexes,[79,80] and if this is indeed the type of EPR signal exhibited by this complex with $\Delta\varphi = 57°$, then in hindsight we can predict that if the EPR spectrum had been recorded at 77 K (as is sometimes the case if the operator is not aware of the relaxation properties of the paramagnetic center), then it is likely that EPR signals only from impurities such as high-spin Fe(III) centers on the surfaces of the crystallites would have been observed. This is because "large g_{max}" (Type I) signals are extremely weak compared to normal rhombic (Type II) signals, as a result of the fact that the transition probability at that maximum g-value depends upon the sum of the squares of the other two g-values divided by the "large g_{max}" value.[126,127] In the case of "large g_{max} species, g_x and g_y are much smaller than for normal rhombic signals, while g_z is much larger, and thus all factors lead to much lower signal intensity for the "large g_{max}" species, for heme b_L about 19% of that of the g_z peak of cytochrome b_5, for b_H about 50%. Hence the signals are weak, even at 4 K, and certainly too weak to observe above 20 K, and often above 10 K; furthermore, they have very different relaxation properties, in that they are much more easily saturated than normal rhombic (Type II) signals. Thus, it is probably in fact a lucky turn of events that the EPR spectrum of this complex was not reported at that time, since it might have been erroneously reported to be a high-spin Fe(III) center, which would have misled scientists about the spin state of this complex. Numerous later attempts to repeat the synthesis of this crystalline form of $[TPPFe(HIm)_2]^+$, with its tantalizing dihedral angle, $\Delta\varphi = 57°$, have invariably failed, and thus even at present we do not know what type of EPR spectrum is exhibited by this complex.

2.4. Covalent Attachment as a Means of Controlling Axial Ligand Plane Dihedral Angle

In the late 1970s this investigator embarked on a 3−4-year synthetic project to create the two geometrical isomers of the six-coordinate TPPFe(III) complexes shown in Figure 6, which she believed would create parallel and perpendicularly oriented imidazole ligand planes. The synthetic route began with the Adler synthesis[128] of the mixture of isomers obtained from a mixture of benzaldehyde and *o*-nitrobenzaldehyde, then separation of isomers (of a total of 13 possible formula, geometrical, and atropisomers), of which the third and fifth were the two *trans*-dinitro-$TPPH_2$ atropisomers and the fourth and seventh were the two *cis*-dinitro-$TPPH_2$ atropisomers.[81] Upon isolation of the trans and cis geometrical isomers (as the combination of the two atropisomeric forms), the nitro groups were reduced to the amino level. Then the desired α,β-atropisomeric diamino forms of each geometrical isomer were isolated by column chromatography, followed by immediate reaction with phosgene, followed by reacton with 2-(*N*-imidazolyl)ethanol, workup, and

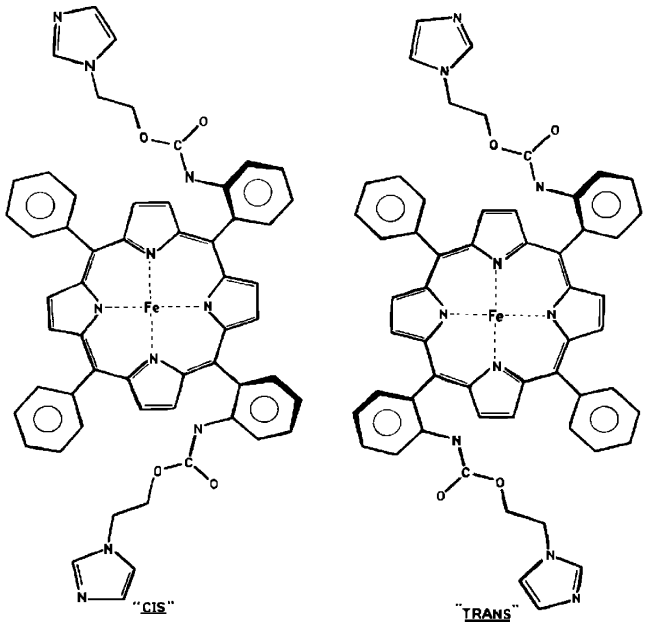

Figure 6. Structures of the six-coordinate iron(III) porphyrinates prepared in this laboratory, abbreviated as $(ImCH_2CH_2OCONH)_2Fe(III)$. The cis isomer was expected to hold the axial ligands in perpendicular and the trans in parallel planes. Note that the heavy lines on the phenyl rings that carry the imidazole arms indicate that one ligand is above (α) while the other is below (β) the plane of the porphyrin ring. Thus these are the α,β atropisomers of the cis and trans geometrical isomers, where both ligands can bind to the iron(III) center. Reprinted from ref 81. Copyright 1984 American Chemical Society.

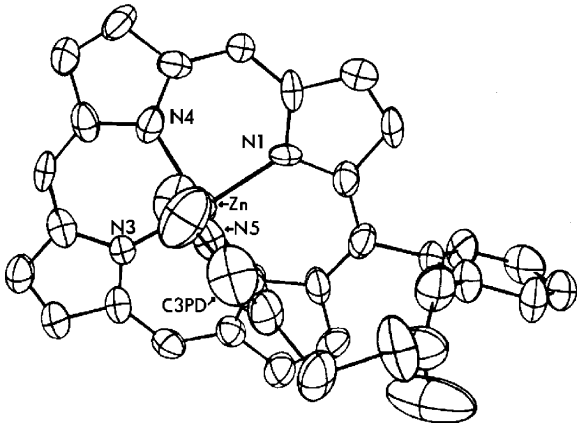

Figure 7. Structure of (*m*-Py-CH_2CH_2CONH)TPPZn(II) showing an ORTEP plot (50% probability ellipsoids) looking down the Py−Zn bond, illustrating the alignment of the pyridine ring and the conformation of the covalent linkage of the arm that attaches the pyridyl ring to the *ortho*-phenyl position of the tetraphenylporphyrin. Reprinted from ref 129. Copyright 1980 American Chemical Society.

insertion of iron. After final workup in the presence of dilute HCl, the samples were dissolved in $CHCl_3$ and a 2.2-fold molar equivalent of triethylamine was added to deprotonate the covalently attached imidazole ligands.[81] Both samples immediately turned red, indicating formation of the low-spin Fe(III) bis-imidazole complexes. EPR spectra of both the cis and trans isomers shown in Figure 6 (meant to create the perpendicular and parallel axial ligand orientations, respectively) at 8 K disappointingly showed the presence of a high-spin Fe(III) signal at $g = 6$ and 2, plus a rather broad normal rhombic signal, but no "large g_{max}" signal.[81]

The single-crystal X-ray determination of the structure of the Zn(II) complex of a related covalently attached pyridine ligand to the ortho position of a phenyl ring of a TPP derivative,[129] obtained at about the same time, showed the reason for this disappointing finding: The amide group, rather than being coplanar and thus in conjugation with the phenyl ring to which it was attached, was rotated nearly 90° to produce a chiral connection between the pyridine ligand and the *ortho*-phenyl group, as shown in Figure 7; the Zn(II)TPP−Py complex had the two resulting diastereomers in the unit cell, each of which had the pyridyl plane lying almost eclipsed with a N_P-Zn-N_P axis ($\varphi = 5.8°$), or rotated ~39° from the expected orientation along the *meso*-*C* axis.[129] With such a large rotation of the ligand plane, then, one would expect that with two covalently attached axial ligands, one on each of two adjacent phenyls (the cis isomer), one could obtain equimolar amounts of parallel and perpendicular ligand orientations, and from the trans isomer one could obtain exactly the same. Furthermore, the attaching arm was one atom longer in the six-coordinate iron porphyrinate (Figure 6)[81] than in the zinc(II) porphyrinate of Figure 7,[129] which would allow even greater flexibility of the imidazole plane orientation. In addition, in a relatively concentrated solution such as that used for EPR spectroscopy, it would be possible for two molecules to share covalently attached ligands to create intermolecular complex dimers in which one iron(III) center has one dangling imidazole ligand and one of its own imidazole ligands bound plus one of the other molecule's imidazole ligands bound at whatever angle it might choose (most likely arranged with the ligand planes nearly parallel to each other, thus giving rise to a normal rhombic EPR signal), while the other iron(III) center has only one ligand bound and thus gives rise to a high-spin Fe(III) EPR signal at $g = 6$ and 2.[81] This project showed that it is extremely difficult to design synthetic model compounds that will do what the designer wants, and what CPK models seemed to show would be the case, rather than what the actual lowest-energy conformation of the molecule dictates the structure should be; at present we have molecular mechanics and density functional theory (DFT) calculational methods to allow us to predict the relative energies of various molecular conformations, but these were not available in the late 1970s. Hence, the idea of holding an axial ligand in a particular and exact orientation by covalent attachment to the porphyrinate ring was abandoned by 1981, the entire six-coordinate porphyrin synthetic effort and its results were summarized briefly in the experimental and discussion sections and one figure (Figure 6 of this review) of our first publication on the EPR spectra of low-spin Fe(III) porphyrinates,[81] and since then our efforts have focused on using steric crowding to help maintain the unusual perpendicular orientation of axial ligand planes.

3. Iron Tetramesitylporphyrinates, A Large Body of Interesting Complexes. The Role of Macrocycle Ruffling

An extensive study of the low-spin Fe(III) and Fe(II) complexes of tetramesitylporphyrin was undertaken by Martin Safo as his Ph.D. project at the University of Notre Dame. Dr. Safo prepared numerous axial ligand complexes and characterized 28 of them structurally by X-ray crystallography, and in collaboration with others by EPR and Mössbauer spectroscopy. This large series of complexes has provided important insights into the structural and magnetic properties of both low-spin Fe(III) and Fe(II) heme centers.

3.1. Non-Hindered Bis-Imidazole Complexes of TMPFe(III)

The understanding of these systems began with an investigation of the TMPFe(III) bis-(1-methylimidazole) and -(4-dimethylaminopyridine) complexes.[87] It was found that the unit cell of $[TMPFe(1\text{-}MeIm)_2]ClO_4$ contains two molecules, each of which has the axial ligands in parallel planes, oriented at angles $\varphi = 23°$ and $\varphi = 36°$ from one of the N_P-Fe-N_P axes. As in the case of the second structure of $[TPPFe(HIm)_2]Cl$ discussed above,[113] the $[TMPFe(1\text{-}MeIm)_2]^+$ molecule with the smaller angle φ shows the larger difference in $Fe-N_P$ bond lengths, with the bond length of those from which the φ angle is measured being 2.002(3) Å, while those nearly perpendicular to the axial ligands are 1.974(2) Å,[87] again, as in the

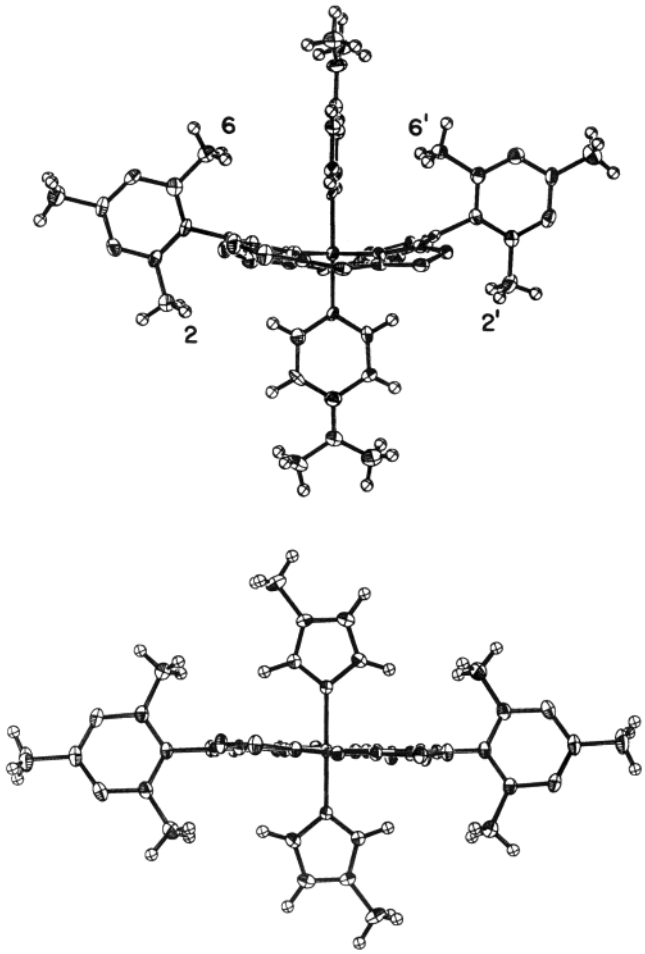

Figure 8. ORTEP diagrams showing the arrangement of the effectively coplanar mesityl rings and the axial ligands in (top) $[TMPFe(4\text{-}NMe_2Py)_2]ClO_4$ and (bottom) $[TMPFe(1\text{-}MeIm)_2]ClO_4$. Hydrogen atoms have been drawn artificially small to improve clarity, and the two mesityl groups of each molecule that are perpendicular to the plane of the figure have been omitted. Reprinted from ref 87. Copyright 1991 American Chemical Society.

$[TPPFe(HIm)_2]^+$ molecules with parallel ligand planes,[113] suggesting a Jahn−Teller distortion due to the unpaired electron preferring to be in the d_π orbital perpendicular to the axial ligands and thus sharing a common nodal plane with them. Another important feature in the structure of these two molecules is that the porphyrinate ring is quite close to planar in both cases, as shown in Figure 8 (bottom) for the $\varphi = 36°$ molecule, but with this molecule having slightly larger deviations of the atoms from the 25-atom mean plane (RMSD = 0.0532 Å) than that with $\varphi = 23°$ (RMSD = 0.0185 Å).[87] As in the case of the second structure of $[TPPFe(HIm)_2]Cl$,[82] two overlapping rhombic EPR signals are observed,[87] but in this case the *g*-values of the two spectra are much more similar, so it is not possible to deconvolute the overlapping signals.

3.2. Bis-Pyridine Complexes of TMPFe(III)

In contrast to the planar $[TMPFe(1\text{-}MeIm)_2]ClO_4$ molecules with parallel ligand planes, the structure of the bis-pyridine complex $[TMPFe(4\text{-}NMe_2Py)_2]ClO_4$ has the axial ligands in nearly perpendicular planes (dihedral angle $\Delta\varphi$ of 79°) with angles $\varphi_1 = -37°$ and $\varphi_2 = 42°$ from the nearest N_P-Fe-N_P axis, and a very ruffled porphyrinate ring, with the deviation of the *meso*-carbons from the 25-atom mean plane, $|\Delta C_m| = 0.51$ Å and a RMSD of 0.3006 Å.[87] This ruffling creates two "grooves", one above and the other below the porphyrinate ring, at 90° angles to each other, which encourage the axial ligands to be in perpendicular planes with $\varphi \sim 45°$, as shown in Figure 8 (top); in this particular molecule, the dihedral angle $\Delta\varphi$ is somewhat less, at 79°, and one of the angles φ is considerably less than 45° (37° in fact).[87] The ruffling of the porphyrinate ring leads to a decrease in the $Fe-N_P$ bond length to 1.964(10) Å, as compared to those of iron(III) porphyrinates with planar porphyrin rings. The two axial ligand bond lengths are slightly different (1.989 and 1.978 Å).[87] In contrast to this structure, the bis-(4-dimethylaminopyridine) complex of OEPFe(III) has axial ligands in strictly parallel planes, with $\varphi = 41°$, and a planar porphyrin ring with a RMSD of 0.0589 Å.[87]

At the time this work was published it was thought that the ruffling of the bis-(4-dimethylaminopyridine) complex of TMPFe(III) was caused by the extension of the 2,6-methyl groups of tetramesitylporphyrin over and under the porphyrin ring, as shown in Figure 8, which caused steric hindrance between these methyl groups and the protons of the pyridine ligands, if they should lie along the meso positions, as they in fact did. This steric hindrance was believed to be responsible for the ruffling of the porphyrinate ring and the "perpendicular" orientation of the 4-dimethylaminopyridine ligands.[87] However, when the Fe(II) analogue of the Fe(III) complex was investigated,[125] it was found that similar axial pyridine ligands are bound to the metal *in parallel planes with large* φ *angles* (40−42°) that place the pyridine ligands quite close to the 2,6-methyl groups. Hence, the reason for the ruffling of the TMPFe(III) complexes of pyridines and hindered imidazoles (to be discussed below) is not steric but is probably electronic in nature.

As expected from the investigation of the $[TPPFe(2\text{-}MeHIm)_2]ClO_4$ complex,[82] the $[TMPFe(4\text{-}NMe_2Py)_2]ClO_4$ complex also gives rise to a "large g_{max}" EPR spectrum, with $g = 3.48$ in the solid state.[87] In fact, perhaps this should not have been expected a priori, for the axial ligands were not in perfectly perpendicular planes. Thus, this complex, with a $\Delta\varphi$ angle of 79°, also exhibits a "large g_{max}" EPR signal, and the question was raised in our minds as to how small the dihedral angle might be and still give rise to this type of EPR signal. (This was one of the many times when unsuccessful attempts were made to synthesize the $[TPPFe(HIm)_2]^+Cl^-\cdot CH_3OH$ of Hoard and coworkers having $\Delta\varphi = 57°$.[113]) The magnetic Mössbauer spectra of this complex allowed estimation of the other two *g*-values, and, depending upon the fit utilized, the value of the tetragonality was either 1.9 or 3.6.[87,130] A tetragonality of greater than 3 for this high-basicity bis-pyridine complex has been found for other Fe(III) porphyrinates,[81,87] and since the axial ligand bond lengths are not longer than expected, the value of 3.6 seems the more reasonable for the

tetragonality. Also notable about the Mössbauer data was that the quadrupole splitting, ΔE_Q, is considerably smaller than has been observed for low-spin Fe(III) porphyrinate complexes having normal rhombic EPR signals (1.75 mm/s as compared to 2.1−2.4 mm/s).[87]

Additional bis-pyridine complexes having lower basicities were then studied, TMPFe(III) complexes in which the axial ligands were 4-NH_2Py, 3-EtPy, 3-ClPy, 3-CNPy, and 4-CNPy.[131] In comparison to 4-NMe_2Py (pK_a of the conjugate acid = 9.7),[87] the quadrupole splittings of the less-basic pyridine ligand complexes become smaller as the basicity decreases (0.97 mm/s for 4-CNPy, with pK_a of the conjugate acid of this pyridine ∼1.1), while the "large g_{max}" EPR feature moves from 3.48 for the 4-NMe_2Py complex[87] to 2.53 for the 4-CNPy complex (but see below), and the ^{1}H NMR spectra also change in a linear manner with the pK_a of the ligand (the pyrrole-H resonance shifts from −30.9 to +2.21 ppm at −80 °C for the series 4-NMe_2Py to 4-CNPy).[131] Nevertheless, all of these complexes have extremely similar molecular structures, with ruffled porphyrinate rings ($|\Delta C_m|$ = 0.36−0.43 Å), large φ angles of 29−44°, and $\Delta\varphi$ angles of 90, 87, and 77° for the 3-EtPy, 4-CNPy, and 3-ClPy complexes, respectively.[131] The Fe−N_P bond lengths in all cases are again shorter (1.961−1.966 Å)[131] than expected for iron porphyrinates having planar porphyrin cores (∼1.988−2.002 Å). Axial bond lengths vary slightly (1.989, 2.002; 2.001, 2.002; 2.018, 2.006 Å, respectively) but non-systematically for the three complexes.[131]

Because the type of EPR signal of the bis-(4-cyanopyridine) complex is not "large g_{max}" but rather axial, with $g_\perp = 2.53$, $g_\parallel = 1.56$, and the pyrrole-H chemical shift at −80° C is not negative, but rather +2.1 ppm, the results for the entire series of complexes were interpreted as being indicative of a smooth change in the electron configuration of the low-spin Fe(III) porphyrinates from $(d_{xy})^2(d_{xz},d_{yz})^3$ toward $(d_{xz},d_{yz})^4(d_{xy})^1$ as the basicity of the pyridine ligand decreases from pK_a of the conjugate acid = 9.7 to 1.1.[131] Study of the MCD spectra of [TMPFe(4-CNPy)$_2$]$^+$ [132] and of the corresponding [TPPFe(4-CNPy)$_2$]$^+$ complex by X-ray crystallography,[133] EPR,[133] Mössbauer,[85,133] and NMR[134] spectroscopies confirmed that the electronic ground state of both of these complexes at low temperatures is the less common $(d_{xz},d_{yz})^4(d_{xy})^1$ electron configuration.

3.3. A Bis-Non-Hindered Imidazole Complex of TMPFe(III) That Crystallizes in Both "Parallel" and "Perpendicular" Forms

In a study of two crystalline forms of [TMPFe(5-MeHIm)$_2$]ClO_4 we found that one form had the axial ligands in approximately parallel planes ("*paral*", $\Delta\varphi$ = 26 and 30° for the two molecules in the unit cell), while the other had the axial ligands in approximately perpendicular planes ("*perp*", $\Delta\varphi = 76°$),[135] but in fact both of these observed dihedral angles are markedly different from the ideal values of 90° for perpendicular and 0° for parallel. The *paral*-[TMPFe-(5-MeHIm)$_2$]$^+$ crystals have two molecules in the unit cell, one of which has $\varphi_1 = -10°$ and $\varphi_2 = 20°$, $\Delta\varphi$ = 30°, with somewhat different axial ligand bond lengths (1.978(6) and 1.961(5) Å, respectively), while the other has $\varphi_1 = -12°$ and $\varphi_2 = 14°$, $\Delta\varphi = 26°$, and more equal axial ligand bond lengths (1.980(5) and 1.985(5) Å, respectively).[135] However, despite the small φ values and the "nearly parallel" ligand arrangement, the former molecule is moderately ruffled ($|\Delta C_m| = 0.16$ Å), while the latter is much less ruffled ($|\Delta C_m| = 0.07$ Å). The Fe−N_P bond lengths are extremely similar for both complexes (1.981−1.983 Å).[135] As for the axial ligands not being in perfectly parallel planes, in some other complexes $\Delta\varphi$ also takes on non-zero angles, such as 11° in [TPPFe-(1-MeIm)$_2$]ClO_4,[136] 6° in [2,6-Cl_2TPPFe(1-VinIm)$_2$]-ClO_4,[137] and 13° in [(Proto IX)Fe(1-MeIm)$_2$]$^+$.[138]

The *perp*-[TMPFe(5-MeHIm)$_2$]$^+$ has individual angles $\varphi_1 = -46°$ and $\varphi_2 = 30°$, $\Delta\varphi = 76°$, and is ruffled ($|\Delta C_m| = 0.32$ Å), slightly more ruffled than the first structure of [TPPFe(HIm)$_2$]$^+$ ($|\Delta C_m| = 0.31$ Å),[114] even though in both cases the five-membered imidazole rings should not require ruffling to avoid contacts of the α-H of the imidazole ligands with the porphyrinate ring. It is also interesting to note that the two axial ligands have different bond lengths, with the one having $\varphi_1 = -46°$ having shorter bond length (1.957(6) Å) than that having $\varphi_2 = 30°$ (1.973-(6) Å).[133] This trend of longer Fe−N_{ax} bonds for smaller values of φ is frequently observed and is the case for the companion structure, *paral*-[TMPFe(5-MeHIm)$_2$]$^+$, molecule A.[135] The planes of the axial imidazoles of *perp*-[TMPFe(5-MeHIm)$_2$]$^+$ are tilted (by 12.5° and 7.6°) from the heme normal. It is probable that crystal packing effects and/or hydrogen-bonding of the non-coordinated 5-MeHIm molecules in the lattice to the N−H proton of the coordinated imidazoles may influence whether the ligands bind in an off-axis manner, since not all mono- and bis-imidazole complexes show this type of distortion. Off-axis binding of imidazole−(histidine) ligands has also been seen in a number of heme proteins.

Molecular mechanics calculations on *paral*- and *perp*-[TMPFe(5-MeHIm)$_2$]$^+$ provided information about the relative stability of these two non-ideal axial ligand plane orientations: it was found that to have two ligands in parallel planes with $\varphi_1,\varphi_2 = 45°$ and a planar porphyrin core is the maximum energy conformation, while having the two ligands in perpendicular planes with $\varphi_1 = -45°$, $\varphi_2 = 45°$ and a ruffled core is the minimum energy.[135] The observed ligand orientation in *perp*-[TMPFe(5-MeHIm)$_2$]$^+$ (φ_1 = −46°, $\varphi_2 = 30°$, $\Delta\varphi = 76°$) has an energy only 0.4 kcal/mol higher than the minimum, as shown in Figure 9.[135] In contrast, assuming a planar porphyrin core, having the axial ligands aligned in parallel planes over the N_P−Fe−N_P axes ($\varphi_1,\varphi_2 = 0°$) also has a high energy.[135] However, having the conformation exhibited by *paral*-[TMPFe(5-MeHIm)$_2$]$^+$ yields a calculated energy of ∼2.6 kcal/mol above the global minimum, and this conformation is close to the local maximum with ligands over a pair of trans Fe−N_P vectors ($\varphi_1,\varphi_2 = 0°$).[135] Thus, the orientations of axial ligands in *paral*- and *perp*-[TMPFe(5-MeHIm)$_2$]$^+$ are within ∼2−3 kcal/mol of each other according to the

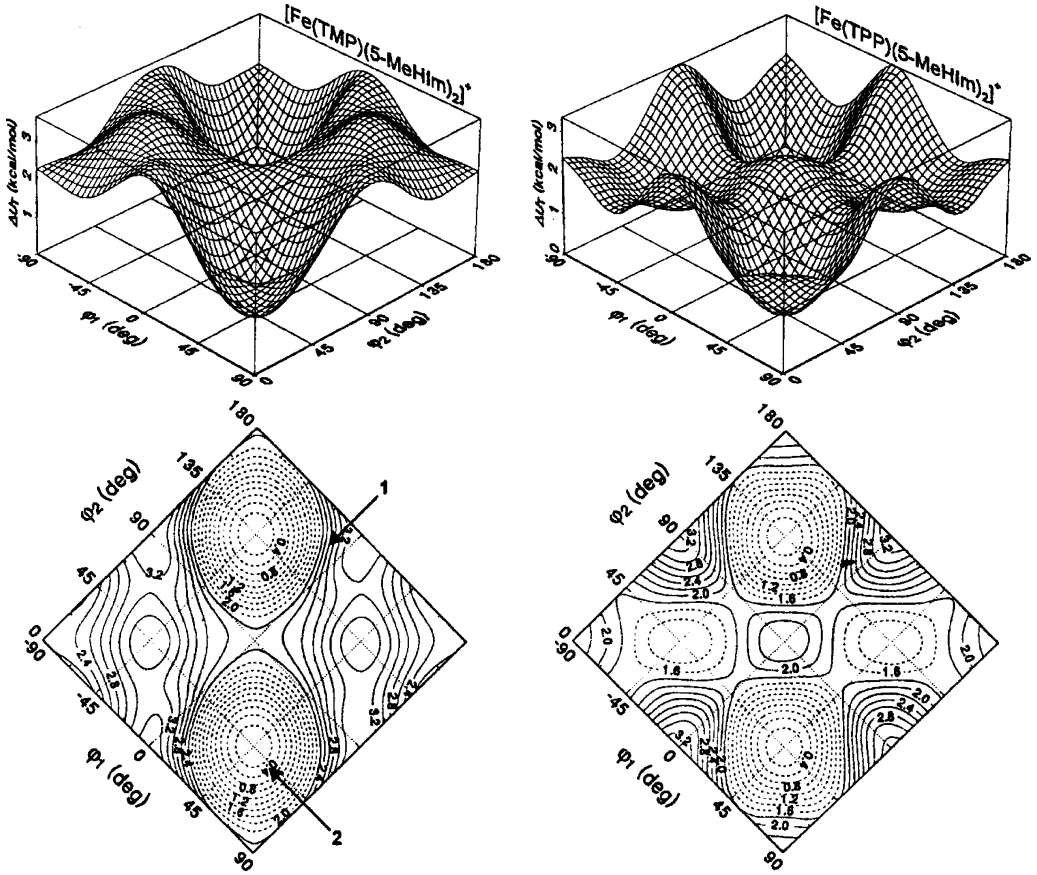

Figure 9. Plot of the change in steric energy (ΔU_T) as a function of axial 5-MeHIm orientation for $[TMPFe(5\text{-}MeHIm)_2]^+$ and $[TPPFe(5\text{-}MeHIm)_2]^+$. A contour map of the three-dimensional surface is shown in each case. φ_1 and φ_2 correspond to the torsion angles $N_P-Fe-N_{ax}-C_{1m}$ for the top and bottom ligands, respectively. The locations of the X-ray structures of $[TMPFe(5\text{-}MeHIm)_2]ClO_4$ on the conformational surface are shown: point 1, *paral*-$[TMPFe(5\text{-}MeHIm)_2]ClO_4$ (molecule A); point 2, *perp*-$[TMPFe(5\text{-}MeHIm)_2]ClO_4$. Reprinted from ref 135. Copyright 1999 American Chemical Society.

molecular mechanics calculations, with the "parallel" being slightly higher in energy. However, for low-spin d^5 systems the "parallel" axial ligand orientation is stabilized by the Jahn−Teller effect by the rhombic splitting of d_{xz} and d_{yz}, $V = 2-3\lambda$, where λ is the spin−orbit coupling constant for low-spin Fe(III). With $\lambda = 400\ cm^{-1}$, or 1.14 kcal/mol, this stabilization is 2.3−3.4 kcal/mol, a stabilization for which molecular mechanics calculations do not account. In this work[135] it was concluded that relative parallel orientation of axial ligands is the apparently preferred orientation for most characterized low-spin Fe(III) porphyrinates having two planar axial ligands, with relative perpendicular orientations being observed only in special circumstances, primarily those of introduced steric effects. The appearance, in the solid state, of ligand orientations approaching the two limiting forms speaks to a near energetic equivalence of conformational isomers. The energy balance between the two forms is the result of crystal field stabilization effects that favor the parallel form, and steric strain effects that favor the perpendicular form.[135] Stabilization energy estimates are so similar for the two that it is easily seen that the energy balance may shift in favor of either conformation, depending on factors such as the degree of ruffling of the porphyrin ring, the nature of the peripheral substituents on the porphyrin ring including the size of the ortho substituents of the *meso*-aryl groups, and variations in the actual dihedral angle, $\Delta\varphi$, between the axial ligand planes.[135]

perp-$[TMPFe(5\text{-}MeHIm)_2]^+$ has a small Mössbauer quadrupole splitting ($\Delta E_Q = 1.78$ mm/s at 120 K) and a "large g_{max}" EPR signal at $g = 3.43$, while *paral*-$[TMPFe(5\text{-}MeHIm)_2]^+$ has a larger quadrupole splitting ($\Delta E_Q = 2.56$ mm/s at 120 K) and a rhombic EPR signal ($g = 2.69$, 2.34−2.43, 1.75) in the crystalline state.[135] These values are similar to those observed in solution: $g = 2.64$, 2.30, 1.80 in DMF:acetonitrile (3:1) glasses at 4.2 K when the ratio of axial ligand to TMPFe(III) is ~60:1, whereas if the axial ligand-to-TMPFe(III) ratio is ~2:1 the *g*-values observed are 2.89, 2.31, and 1.58.[135] The latter EPR values lead to tetragonality = 3.22 and rhombicity = 0.64 (Table 2), values very typical of ferriheme centers bound to neutral imidazoles (Figure 1, type B), while the former solution EPR values lead to tetragonality $\Delta/\lambda = 4.09$ and rhombicity $V/\Delta = 0.76$, values very typical of ferriheme centers bound to one imidazolate anion and one neutral imidazole.[139] The *g*-values observed for the crystalline sample are also much more similar to those of mixed imidazolate−imidazole-ligated complexes, and it is interesting to note that one of the 5-MeHIm ligands is hydrogen-bound to a 5-MeHIm molecule in the lattice in this structure, thus probably imparting partial imidazolate character to that ligand in each of the molecules in the unit cell.[135]

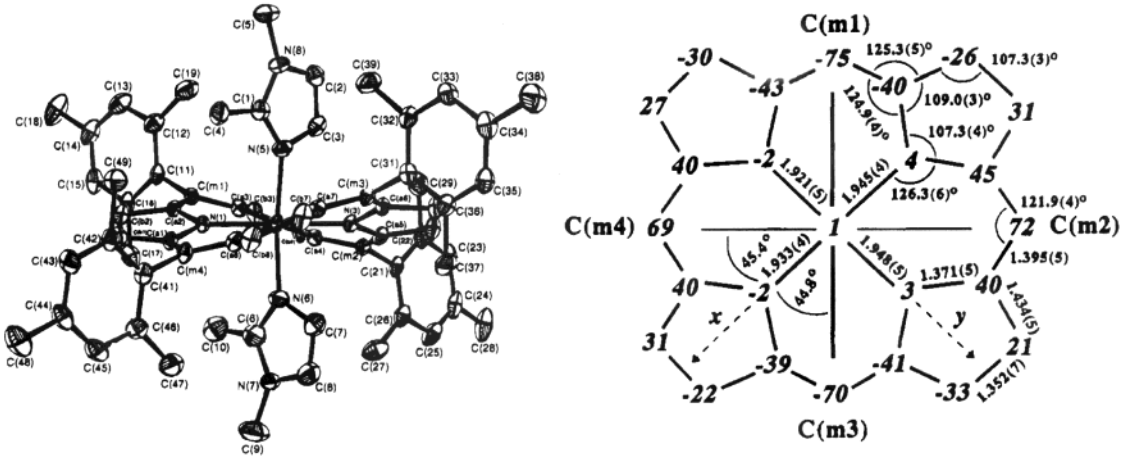

Figure 10. (A) ORTEP diagram of the structure of the $[TMPFe(1,2\text{-}Me_2Im)_2]^+$ cation. Fifty percent probability surfaces are shown. Hydrogen atoms have been omitted for clarity. (B) Formal diagram of the porphinato core of $[TMPFe(1,2\text{-}Me_2Im)_2]ClO_4$ displaying the perpendicular displacement, in units of 0.01 Å, of each atom from the mean plane of the 25-atom core. Averaged values for the chemically unique bond distances (in Å) and angles in the porphinato core are shown. The orientations (and angles φ_1 and φ_2) of the axial ligands relative to the Fe−N(4) bond vector are indicated by the heavy line for the above-plane ligand and the thinner line for the below-plane ligand. Individual values of the $Fe-N_P$ bond distances are given, along with the **x**- and **y**-vectors defining the Cartesian axes of the heme group. Reprinted from ref 140. Copyright 1995 American Chemical Society.

3.4. The Bis-1,2-Dimethylimidazole Complex of TMPFe(III)

By far the most ruffled of the TMPFe(III) complexes having perpendicular axial ligand planes is the bis-(1,2-dimethylimidazole) complex, $[TMPFe(1,2\text{-}Me_2Im)_2]ClO_4$.[140] In this case the *meso*-carbon deviation from the mean plane of the porphyrin ring, $|\Delta C_m| = 0.72$ Å, the largest value yet observed, and the $Fe-N_P$ bond length is 1.937 Å, the shortest yet observed. The angle $\varphi_1 = -44.8$ and $\varphi_2 = 45.4°$, yielding a dihedral angle $\Delta\varphi = 90°$,[140] as shown in Figure 10.

The Mössbauer quadrupole splitting $\Delta E_Q = 1.25$ mm/s at 250 K (very broad at 4.2 K)[140] is somewhat smaller than those of $[TMPFe(2\text{-}MeHIm)_2]^+$ (1.48 mm/s)[131] and $[TPPFe(2\text{-}MeHIm)_2]^+$ (1.77 mm/s),[82] but within the range of the bis-pyridine ligand complexes of TMPFe(III).[131] The EPR spectrum was not reported in that work, but the corresponding bis-(2-MeHIm) complex has a "large g_{max}" feature at $g = 3.17$.[131] The smaller g-value in this case than observed for $[TPPFe(2\text{-}MeHIm)_2]^+$ (3.41)[82] suggests a tendency for strongly ruffled porphyrinates to have the less-common $(d_{xz},d_{yz})^4(d_{xy})^1$ electron configuration, even if the axial ligand is a high basicity pyridine or imidazole, and we predict that the actual g_{max} value for $[TMPFe(1,2\text{-}Me_2Im)_2]^+$ is smaller than 3.17. Nakamura and co-workers later showed that by encouraging greater (expected) ruffling on the porphyrin ring by introducing bulkier substituents R on the 2,6-phenyl positions of TPPFe(III), the g-values of the bis-ligand complexes (2-MeHIm and benzimidazole) shift to lower values, with the smallest g-value being 2.89 for $[TMPFe(benzimidazole)_2]^+$ and the smallest g-value for a bis-(2-MeHIm) complex being 3.08, for R = isopropyl.[141] More recently, this investigator has also studied a series of *meso*-tetraalkylporphyrinatoiron(III) complexes of 2-methylimidazole and found that for alkyl = isopropyl this complex has a g_{max} value as low as 2.58.[142] Hence, strong ruffling of the porphyrinate ring, with axial ligands in perpendicular planes, even when strongly σ- and π-donating axial ligands such as hindered imidazoles are bound to Fe(III), increases the tendency for the electron configuration to be $(d_{xz},d_{yz})^4(d_{xy})^1$, and there appears to be a continuum that connects ruffled complexes having "large g_{max}" EPR signals with $g \geq 3.2$ to those having axial EPR signals with $g_{max} \leq 2.6$. These have recently been called Type I and Type III low-spin Fe(III) porphyrinate centers, respectively.[84]

Thus, with this work on TMPFe(III) complexes and the previous findings based on TPPFe(III) complexes, it had been established that for these models of the membrane-bound, bis-histidine-coordinated cytochromes *b* of Complexes II and III, "large g_{max}" EPR signals are observed when the axial ligands are in "perpendicular" planes, where $\Delta\varphi$ can be strictly 90° or as small as 76°, and that rhombic EPR signals are observed when the axial ligands are in "parallel" planes, where $\Delta\varphi$ can be strictly 0° or as large as 30°.[135] The complexes having "perpendicular" axial ligand planes are invariably ruffled for TMPFe(III), TPPFe(III), and other *meso*-only-substituted model ferrihemes, including those having alkyl substituents on the *meso*-carbons.[143,144] As we will see below, the ruffling is a problem if these complexes are to be used as models of the membrane-bound cytochromes *b*.

3.5. Bis-Pyridine and -Imidazole Complexes of TMPFe(II)

A detailed investigation of the Fe(II) counterparts of some of these TMPFe(III) complexes[125] provided some extremely interesting and important information about their ability to model the geometric and electronic properties of the bis-histidine-coordinated cytochromes *b* of mitochondrial Complexes II and III. The TMPFe(II) complexes of 4-CNPy, 3-CNPy, 3-MePy, Py, 4-NMe_2Py, 3-ClPy, and 1-MeIm were prepared and the first three were characterized by X-ray

crystallography.[125] All of these complexes were also characterized by Mössbauer spectroscopy. It was found that in all cases for which single crystals were obtained, the axial ligands of these Fe(II) tetramesitylporphyrinates are in exactly parallel planes (the complexes have inversion centers) having large angles, $\varphi = 40-42°$, almost perfectly planar porphyrinate cores having small RMSD from the 25-atom mean plane of 0.025−0.038 Å, and small Mössbauer quadrupole splittings ($\Delta E_Q = 1.09-1.24$ mm/s at 4.2 K).[125] Other related complexes, including [TMPFe(1-VinIm)$_2$][124] and TPPFe(II) complexes of 1-VinIm[124] and 1-SiMe$_3$Im,[124] also have $\Delta E_Q = 1.00-1.03$ mm/s at 4.2 K, and the TPPFe(II) complexes of 1-BzlIm,[124] 1-AcIm,[124] 1-MeIm,[124] and Py,[145] as well as [OEPFe(Py)$_2$],[146] (Proto IX)Fe(II) complexes of 1-MeIm,[147] HIm,[147] and Py,[146] and ferrocytochrome b_5[147] have $\Delta E_Q = 0.97-1.21$ mm/s at 77 K. In contrast, when Arizona undergraduate Joshua L. Wright carried out a summer research project on Mössbauer spectroscopy of low-spin Fe(II) porphyrinate complexes that had bulky axial ligands in the laboratory of Professor Alfred X. Trautwein in Lübeck, he found that there were some Fe(II) porphyrinates that had different Mössbauer parameters, those being the TMPFe(II) complexes of hindered imidazoles (2-MeHIm and 1,2-Me$_2$Im), as well as [OEPFe(2-MeHIm)$_2$]. The values of ΔE_Q obtained for these complexes in dimethylacetamide solution at 77 K were 1.64−1.73 mm/s,[148] much larger than those observed for all other bis-ligand complexes of Fe(II) porphyrinates that had been reported previously.[124,125,145−147] Molecular orbital calculations of the quadrupole splitting of [TMPFe(2-MeHIm)$_2$] in the local density approximation, using the self-consistent-charge-Xα method,[149] could only reproduce the 4.2 K quadrupole splitting value (refined as 1.61 mm/s) if it were assumed that the structure of the Fe(II) complex was identical to that of the related Fe(III) complex, [TMPFe(1,2-Me$_2$-Im)$_2$]$^+$,[140] i.e., with a very ruffled porphyrinate core. Thus, this calculation suggested that the Fe(II) porphyrinate bis-ligand complexes of hindered imidazoles, which could only be formed at very low temperatures, have ruffled cores.

At about the same time, we showed by ^{1}H NMR spectroscopy[150,151] that at very low temperatures (200 to 178 K), the [TMPFe(1,2-Me$_2$Im)$_2$] complex is stable with respect to dissociation of the axial ligands and that, from the multiplicity of NMR resonances observed for the *ortho*-methyl groups of the TMP (four *o*-CH$_3$ signals), the 1,2-Me$_2$Im ligands must be in perpendicular planes, as had previously been shown for the Fe(III) analogue.[121,122] Because of the instability of this and related complexes at ambient temperatures, no structure of a bis-hindered imidazole complex of TMPFe(II) or any other *meso*-only-substituted Fe(II) porphyrinate has yet been determined.

3.6. Electrochemical Results: Interrelating Fe(III) and Fe(II) Complexes through the Redox Reaction

Although no structures of TMPFe(II) complexes with hindered imidazoles have been determined, the stability constants for these complexes at ambient temperatures could be measured in favorable cases by electrochemical methods.[152] These methods involve measuring the $E_{1/2}$ values for the Fe^{III}/Fe^{II} and Fe^{II}/Fe^{I} waves by cyclic voltammetry as a function of the concentration of axial ligand and then fitting the ligand concentration dependence of the reduction potential observed for each half-reaction to the full Nernst equation,

$$(E_{1/2})_c = (E_{1/2})_s - (RT/nF)\ln\{(1 + \beta_1^{III}[L] + \beta_2^{III}[L]^2)/(1 + \beta_1^{II}[L] + \beta_2^{II}[L]^2)\} \quad (3)$$

where $(E_{1/2})_c$ is the reduction potential measured for the complex at each concentration of axial ligand, $(E_{1/2})_s$ is the reduction potential measured for the iron porphyrinate in the absence of added ligand, [L] is the equilibrium concentration of axial ligand, and the β_n are the overall equilibrium constants for the binding of one ($n = 1$) or two ($n = 2$) axial ligands to Fe(III) and Fe(II) (for the Fe^{III}/Fe^{II} wave) or Fe(II) and Fe(I) (for the Fe^{II}/Fe^{I} wave). Thus, for example, $\beta_1^{III} = K_1^{III} = [PFe^{III}L]/[PFe^{III}][L]$ and $\beta_2^{III} = K_1^{III}K_2^{III} = [PFe^{III}L_2]/[PFe^{III}][L]^2$, where all concentrations are those at equilibrium. (Overall charges on the complex have been omitted for simplicity.) In many cases $\beta_1^{III}[L] \ll \beta_2^{III}[L]^2 \gg 1$, and the analogous situation holds for $\beta_1^{II}[L]$ and $\beta_2^{II}[L]^2$, so that eq 3 can be simplified to

$$(E_{1/2})_c = (E_{1/2})_s - (2.303RT/nF)\log\{\beta_p^{ox}/\beta_q^{red}\} - (2.303RT/nF)\log[L]^{p-q} \quad (4)$$

for the Fe^{III}/Fe^{II} wave, where p and q may be 0, 1, or 2 for these metalloporpyrinates. Likewise, for the Fe^{II}/Fe^{I} wave, in many cases the binding of axial ligands to the Fe(I) oxidation state over the concentration ranges utilized for these studies could not be detected, and eq 3 in that case reduces to

$$(E_{1/2})_c = (E_{1/2})_s - (2.303RT/nF)\log\beta_p^{ox} - (2.303RT/nF)\log[L]^p \quad (5)$$

In such cases, $\log \beta_2^{II}$ can be directly determined from the concentration dependence of the Fe(II)/Fe(I) potential using eq 5, and then this value can be utilized in eq 4 with reduction potential data for the Fe^{III}/Fe^{II} couple, where $\log \beta_2^{III}$ is then the only unknown. In some cases, however, it was necessary to use the full eq 3.[152] An example of the data obtained for the case of $\beta_2^{II} > \beta_2^{III}$ is shown in Figure 11, and some of the equilibrium constants obtained in this study[152] are presented in Table 3.

Also presented in Table 3 are the observed reduction potentials (vs SCE) for the Fe^{III}/Fe^{II} couple in the presence of a concentration of the axial ligand that is high enough to fully complex both oxidation states (i.e., $p - q = 0$ in eq 4). These reduction potentials, then, measure the relative stability of the bis-axial ligand complexes of the two oxidation states, in terms of $\log \beta_2^{III}/\beta_2^{II}$, and should be directly comparable to the reduction potentials of the bis-histidine-coordinated cytochromes *b* of mitochondrial inner membrane Complexes II and III, Table 1. The

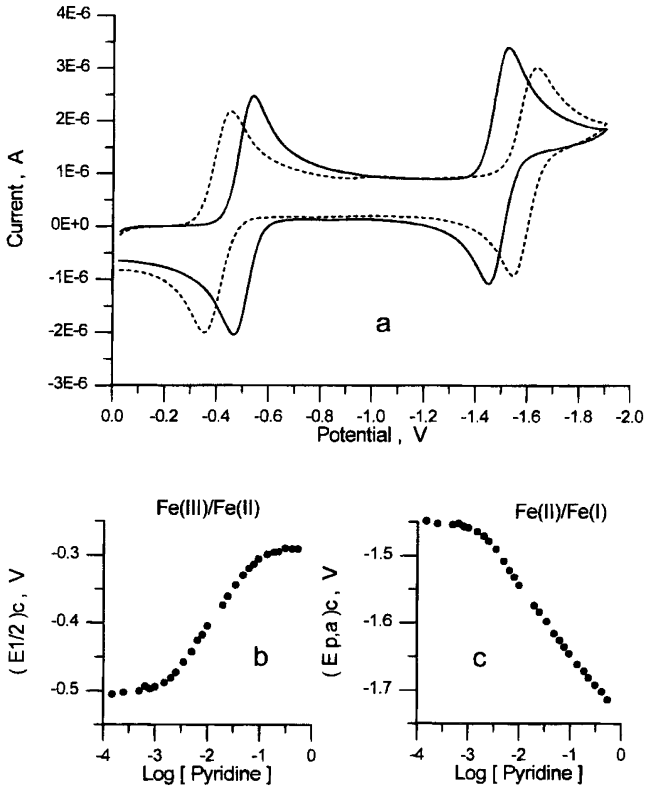

Figure 11. Example of redox couple shifts during titration and the dependence of $E_{1/2}$ on log [L] for the case $\beta_2^{II} > \beta_2^{III}$. The system shown is that of $TPPFeClO_4$ (1.0 mM) and pyridine in dimethylformamide (0.1 M TBAP). (a) Ligand concentrations: solid line, no pyridine; dashed line, [Py] $= 1.9 \times 10^{-2}$ M. All measurements were made at 25 °C with a scan rate of 50 mV/s. (b) Plot of eq 4 (Fe^{III}/Fe^{II} couple) and (c) plot of eq 5 (Fe^{II}/Fe^{I} anodic peak) for the complete set of titration data. Reprinted from ref 152. Copyright 1996 American Chemical Society.

conversion between the SHE and SCE reference electrode scales is $E_{SHE} = E_{SCE} + 242$ mV, although this calculation may provide somewhat artificial comparisons because of the difference in solvent utilized for the model heme studies (DMF).[152] The column in Table 3 labeled $(E_{1/2})_{2-MeHIm} - (E_{1/2})_L$ compares the potential difference between a system in which both Fe(III) and Fe(II) must have the axial ligands in perpendicular planes and a system in which the Fe(II) complex is known to have its axial ligands L in parallel planes, while the Fe(III) complex is known to have its axial ligands L in either parallel (1-MeIm) or perpendicular (4-NMe_2Py in all but the TPPFe complex) planes. Aside from the obvious effect of ligand basicity on the values of log β_2^{III} (pyridines of various basicities[152]), these data lead to the conclusion that having the axial ligands in perpendicular planes, at least if they are constrained to be over the *meso*-carbons of the iron porphyrinate, as is true of all of the *meso*-tetraphenylporphyrinates of iron, causes a negative shift in the reduction potential for the Fe^{III}/Fe^{II} couple *because* the value of log β_2^{II} is about two (1.8−2.5) units smaller for 2-MeHIm than for ligands that can bind to Fe(II) in parallel planes. (But these same values of log β_2^{II} suggest the conditions under which the Fe(II) complexes of 2-MeHIm would have to be crystallized—in the presence of 15−25 mM excess 2-MeHIm in the mother liquor. However, the problem of the dynamics of the system still remains (ligand on−off kinetics, inversion of the ruffled porphyrin core) and could still prevent formation of crystals, unless a particular crystal form is very insoluble.) Because the reduction potentials of the membrane-bound proteins being modeled are more positive, rather than negative, than those in which the axial ligands are known to be in parallel planes, it thus appeared that these meso-substituted synthetic hemes were not good models of the cytochromes *b* of mitochondrial Complexes II and III.

As a part of our attempt to understand the reduction potentials of these model hemes that are based upon the TPP skeleton, in most cases having ortho substituents on the phenyl rings,[152] we prepared and investigated a large number of unsymmetrically substituted complexes that had in common three *meso*-(*p*-methoxyphenyl) groups and one uniquely substituted *meso*-phenyl group, for example, (2,6-Br_2)(4-OCH_3)$_3$TPPFeCl, and examined their NMR and EPR spectra, their equilibrium constants for

Table 3. Electrochemical Data for the Fe^{III}/Fe^{II} Couple of Synthetic Heme Complexes[152]

iron porphyrin	ligand	$E_{1/2}$, mV vs SCE	$(E_{1/2})_{2-MeHIm} - (E_{1/2})_L$, mV	log β_2^{II}	log β_2^{III}
TPPFe	none	+33			
	4-NMe_2Py	−47		6.7	6.8
	1-MeIm	−89		6.5	7.2
	4-$MeIm^-$	−750[a]			
	2-MeHIm	*b*			
TMPFe	none	−96			
	4-NMe_2Py	−121	−91	7.9	8.3
	1-MeIm	−130	−82	7.3	7.9
	2-MeHIm	−212		5.5	7.4
(2,6-Cl_2)TPPFe	none	−13			
	4-NMe_2Py	−11	−104	8.4	8.4
	1-MeIm	+3	−118	7.4	7.1
	2-MeHIm	−115		5.6	7.3
(2,6-Br_2)TPPFe	none	−40			
	4-NMe_2Py	−39	−92	>9	>9
	1-MeIm	−40	−91	7.7	7.7
	2-MeHIm	−131		5.2	6.7

[a] From ref 120. Solvent = dimethylacetamide. [b] Fe(II) bis-ligand complex cannot be fully formed, so the limiting potential cannot be measured.

ligand binding, and some of their reduction potentials. It was found that *ortho*-halogens and the CF_3 group behave as electron-donating substituents, in that they stabilize the formation of the cationic product of bis-ligand complex formation, for example, $[(2,6\text{-}Br_2)(4\text{-}OCH_3)_3TPPFe(1\text{-}MeIm)_2]^+Cl^-$; all 2,6-halogen-substituted phenyl groups have this characteristic, but the larger the halogen (Br > Cl > F), the larger the equilibrium constant for ligand addition to the Fe(III) form.[153] The effect is smaller for the Fe(II) complexes. This effect was interpreted as indicating a transfer of electron density from the ortho substituents directly to the porphyrinate ring by overlap of the electron clouds of the ortho substituent and the π system of the porphyrin,[153] which thus stabilizes the formal positive charge on the Fe(III) bis-ligand complexes. Later DFT calculations showed that this overlap of electron clouds can explain the donation of electron density of *ortho*-halogens to the porphyrinate ring in tetraphenylporphyrins.[154]

3.7. Conclusions Reached from Investigations of Structures and Redox Properties of Iron Tetraphenyl- and Tetramesitylporphyrinates, and Their Implications

A tacit assumption of our original calculation[82] of the expected difference in reduction potential for hemes with axial ligands in parallel and perpendicular planes was that there would be no difference in energy of the two possible forms in the reduced state, since all three t_{2g}-type orbitals are fully populated. However, if both parallel and perpendicular orientations of low-spin Fe(II) hemes had equal energy, we would expect to observe as many (or at least *some*) examples of perpendicularly aligned axial ligand planes as parallel, which is not the case. Furthermore, as mentioned above, the only mono-heme water-soluble ferricytochrome *c* that is bis-histidine ligated with the imidazole planes believed to be perpendicular to each other loses one of the histidines to become a high-spin heme center upon pH-linked reduction to Fe(II).[109] All Fe(II) model hemes investigated thus far have been found to have their axial ligands lying over the meso positions ($\varphi \approx 45°$) if those ligands are pyridines,[124,125] and at any angle, including over or near the porphyrin nitrogens ($\varphi \approx 0-10°$), if the ligands are non-hindered imidazoles,[124] in parallel planes in both cases. There is no obvious electronic reason why low-spin d^6, for which the d_π orbitals are both filled, should favor parallel alignment of axial ligand planes. In fact, we had thought that if the axial ligands were in perpendicular planes, then to the extent that these ligands were π acceptors, one ligand could interact by M→L π-backbonding from the d_{xz} orbital of low-spin Fe(II) while the other ligand interacted similarly with the d_{yz} orbital. Nevertheless, both π-donor and π-acceptor ligand complexes have these ligands in parallel planes,[124,125] so this is the preferred geometry for Fe(II) porphyrinates. As mentioned above in section 3.5, only in the case of the bis-(1,2-dimethylimidazole) complex of TMPFe(II) have we obtained evidence (Mössbauer[149] and NMR[150,151] spectroscopy) that at very low temperatures (200 to 4.2 K) the axial ligands can be stabilized in perpendicular planes. Hence, for complexes in which axial ligands lie over the meso positions of the porphyrin ring, there appears to be a large energy barrier to having the axial ligands in perpendicular planes *for Fe(II)*, while Fe(III) *prefers* having axial ligands in perpendicular planes if there is any steric interference between porphyrin substituents and axial ligands (but if there is no steric interference, Fe(III) also prefers to have axial ligands in parallel planes). We hypothesized that the energy barrier in the case of Fe(II) complexes might be due to the necessity of ruffling the porphyrin in order for axial ligands to lie in perpendicular planes over the meso positions.[149] However, mammalian cytochromes *c* have very ruffled porphyrin rings with the histidine imidazole plane lying over the α,γ-meso positions,[45,46,57,155-157] yet ligand binding in the Fe(II) state is very strong, stronger than in the Fe(III) state, as evidenced by the positive reduction potentials of mammalian cytochromes *c*.

It is unlikely that the bis-histidine-coordinated cytochromes *b* of mitochondrial Complexes II and III and chloroplasts in their native, membrane-bound forms change the orientation of their axial histidine ligands upon oxidation/reduction. This assertion is made on the basis of the finding that the histidine imidazole plane orientations found in most heme proteins are stabilized not only by the packing of protein side chains within the heme pocket, but also by covalent attachment of the histidine imidazole side chain to the protein backbone and by hydrogen-bonding of the imidazole N−H to protein residues.[34,158-160] Because the perpendicular arrangement of axial ligand planes in low-spin Fe(III) hemes is disfavored by the Jahn−Teller effect,[115] and since we observe experimentally that non-hindered imidazole ligands prefer to bind to model hemes in parallel planes at low temperatures,[82] it appears that nature must have chosen to provide a protein pocket and a histidine N−H hydrogen-bonding network that stabilizes the perpendicular orientation in these membrane-bound cytochromes *b*. It also seems unlikely that this hydrogen-bonding framework is broken each time reduction takes place and then re-formed upon reoxidation. The expectation, based upon the small equilibrium constants for bis-2-MeHIm complex formation by Fe(II) porphyrinates[152] and the interrelationship between the ratio of the binding constants for the two oxidation states and the reduction potential via the Nernst equation,[152] is that complexes in which ligands are forced to be in perpendicular planes over the meso positions should have more negative reduction potentials than those having ligands in nearly parallel planes. Whether the same would be true of complexes having axial ligands in perpendicular planes over the porphyrin N−Fe−N axes, where ruffling should be minimized, had not been investigated before 2001. We thus considered it important to prepare model hemes in which the axial ligands are in nearly perpendicular planes in both the oxidized and reduced states in order to gain an understanding of the spectroscopic and redox properties of this geometry and why nature chooses

to create it in certain cases (mitochondrial Complexes II and III cytochromes *b* and chloroplast cytochrome b_6) and not others (cytochromes b_5, b_2). The preparation and investigation of this new class of model ferriheme complexes is discussed in the next section.

4. Iron Octaalkyltetraphenylporphyrinates: The Use of Saddled Macrocycles as Models of the Cytochromes

To prepare synthetic metal complexes that accurately model metal centers in proteins is in general quite challenging, mainly because small molecules usually have the ability to adopt whatever geometry gives rise to the minimum energy of the system in the absence of protein constraints. Covalent attachment of axial ligands tends to leave more flexibility than desired, as discussed above in section 2.4. Thus, to find model hemes in which axial ligands could be stabilized in perpendicular planes for both Fe(III) and Fe(II), we felt that we should seek synthetic porphyrins that could stabilize the binding of axial ligands with their planes near the N_P-Fe-N_P axes (small φ angles), which should thus have little tendency to be ruffled. Our reasoning was that because the existing structures of the cytochromes *b* of mitochondrial Complexes II and III had not yet been refined to less than 2.2 Å, it was possible that further refinement might show that the axial ligand planes lay close to the porphyrin nitrogens rather than the meso positions, and that this type of structure might be amenable to having the axial ligands in nearly perpendicular planes for both oxidation states, since ruffling should not take place, or at least not to the same extent. Published molecular mechanics investigations of several six-coordinate Co(III) complexes of dodecasubstituted porphyrinates such as octaethyltetraphenylporphyrin $[OETPPCo(L)_2]^+$ indicated that the lowest energy structures of these complexes had small φ angles ($\varphi = 10-14°$ for pyridine, 2° for imidazole ligands) and highly saddled, not ruffled, porphyrinate cores.[161] Thus, we began an investigation of several axial ligand complexes of OETPPFe(III).[162] The structure of the bis-2-MeHIm complex showed that the axial ligands are in perpendicular planes with $\varphi = 14°$ and $|\Delta C_m| = 0.09$ Å, indicating a very small ruffling component to the porphyrin core conformation. However, the porphyrin nitrogens alternate above and below the mean plane of the 25-atom core by 0.10 Å, and the β-pyrrole carbons of a given pyrrole ring are 1.20 and 1.23 Å above or below the mean plane,[162] as shown by the formal core diagram in Figure 12. Hence, this complex is highly saddled, with only a small ruffling component, and the axial ligands are in perpendicular planes with small φ. Consistent with the perpendicular arrangement of axial ligand planes, the complex exhibits a "large g_{max}" EPR signal at $g = 3.26$.[162]

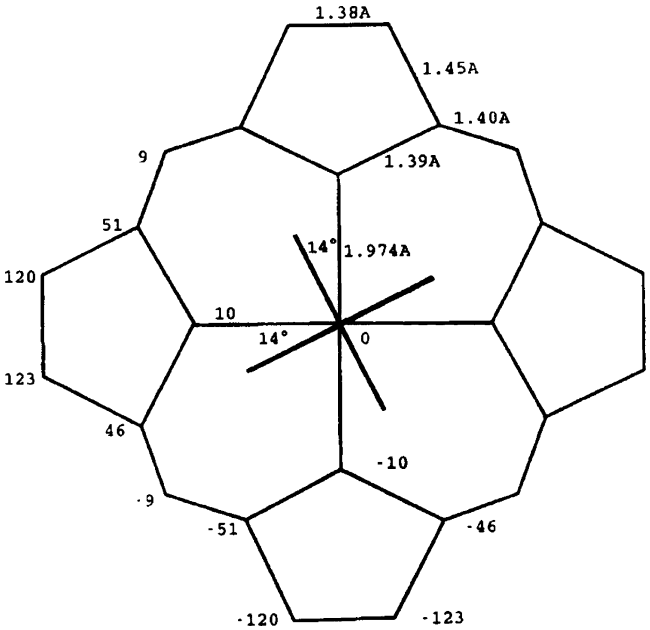

Figure 12. Average bond distances in $[OETPPFe(2\text{-}MeHIm)_2]^+$, displacements Δ from the average of the 25-atom porphyrin core in units of 0.01 Å, and axial ligand plane orientations. Reprinted from ref 162. Copyright 2001 American Chemical Society.

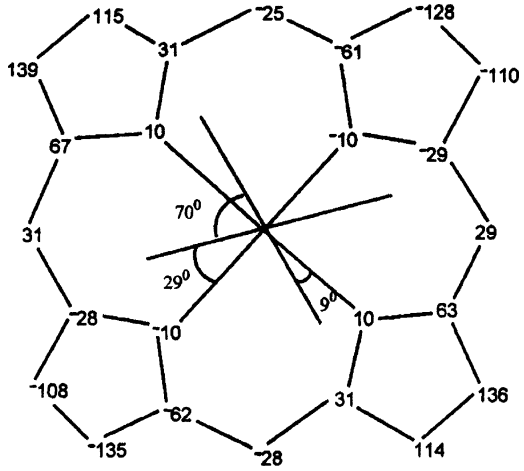

Figure 13. Displacements Δ from the average of the 25-atom porphyrin core of $[OETPPFe(4\text{-}NMe_2Py)_2]^+$, in units of 0.01 Å, and axial ligand plane orientations. Reprinted from ref 162. Copyright 2001 American Chemical Society.

4.1. The Bis-(4-Dimethylaminopyridine) and -(1-Methylimidazole) Complexes of OETPPFe(III)

For the bis-(4-dimethylaminopyridine) complex of OETPPFe(III), one pyridine ligand was found to be lying nearly over the N_P-Fe-N_P axis ($\varphi_1 = 9°$), while the other is rotated 61° in the opposite direction from the same axis, thus yielding a dihedral angle $\Delta\varphi = 70°$.[162] A "large g_{max}" EPR spectrum is also observed for the crystals of this complex.[162] This complex exhibits less saddling but more ruffling than the 2-MeHIm complex, as shown in the formal core diagram of Figure 13, and may be near the transition state for ligand rotation/porphyrin core inversion.[162] When the non-bulky ligand, 1-methylimidazole, is used instead, two EPR signals are obtained for the frozen CH_2Cl_2 solution complex, a "large g_{max}" (Type I) signal and a normal rhombic (Type II) signal,[162] as shown in Figure 14. Observation of a Type II EPR signal suggests a large driving force for Fe(III) to have its ligands in "parallel" planes, and we estimated (molecular mechanics) that it would cost only about 1 kcal/mol to allow the unhindered imidazole

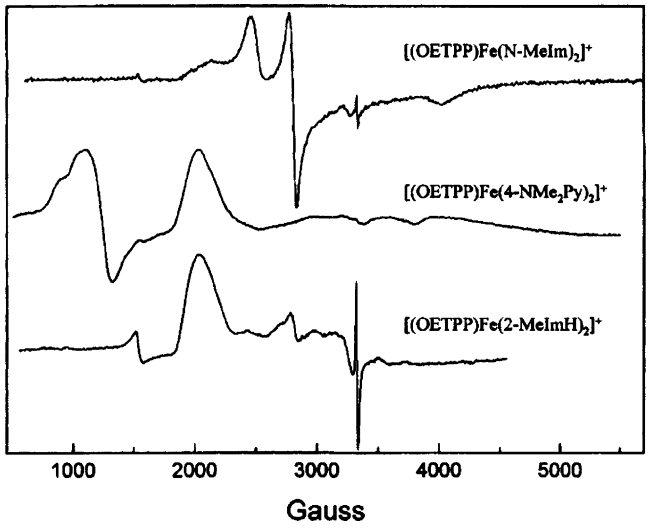

Figure 14. EPR spectra of $[OETPPFe(1\text{-}MeIm)_2]^+$ (top) in frozen CD_2Cl_2 ($g = 3.12$ for the "large g_{max}" signal and $g = 2.72$, 2.38, and 1.66 for the normal rhombic signal), $[OETPPFe(4\text{-}NMe_2Py)_2]^+$ (middle) in the solid state ($g = 3.29$ for the major peak near 2000 G), and $[OETPPFe(2\text{-}MeHIm)_2]^+$ (bottom) in methylene chloride at 4.2 K ($g = 3.26$ for the major peak near 2000 G). For the middle spectrum, a large high-spin Fe(III) signal is also observed at $g = 6$ and 2, while for both frozen solution spectra, free radical impurity signals are seen at $g = 2$. All spectra were recorded at 4.2 K. Reprinted from ref 162. Copyright 2001 American Chemical Society.

ligands to rotate by 15° (and indeed, even the bis-(2-MeHIm) complex has the ligands rotated by 14°).[162] If the two ligands rotate in the same direction, each by 15°, then the resultant angle between the two ligands would remain 90°, while if the two rotate in opposite directions by the same amount, the resultant angle would be 60°. Larger angles of rotation could be achieved at correspondingly greater energy cost, which, up to a point, could be offset by the energy stabilization due to the Jahn−Teller effect[115] when the dihedral angle is small.

Finding a system that exhibits both types of EPR signals in a glassy sample was an extremely important serendipity. The next step was to attempt to crystallize this $[OETPPFe(1\text{-}MeIm)_2]^+$ complex. This has turned out to be an extremely interesting, yet challenging, system. Thus far, two crystalline forms have been obtained, one of which has a sharp "large g_{max}" EPR signal at $g = 3.27$,[163] as shown in Figure 15a. Upon standing for several days at room temperature in the EPR tube, the crystals changed from shiny crystallites to oil and then to dull powder, and the clean "large g_{max}" EPR signal at $g = 3.27$ obtained immediately after harvesting the crystals (Figure 15a) was replaced by an overlapping EPR signal composed of a slightly shifted "large g_{max}" signal ($g = 3.14$) plus a normal rhombic EPR signal with $g = 2.75$, 2.36, 1.62 (Figure 15b),[163] values essentially identical to those obtained in frozen CD_2Cl_2 solution[162] (Figure 14).

The solution of the structure of the freshly harvested crystals (protected by a layer of mother liquor) proceeded well for this crystalline form of *perp*-$[OETPPFe(1\text{-}MeIm)_2]^+$, which shows it to belong to the space group $P2_1$, and to be a very well-behaved

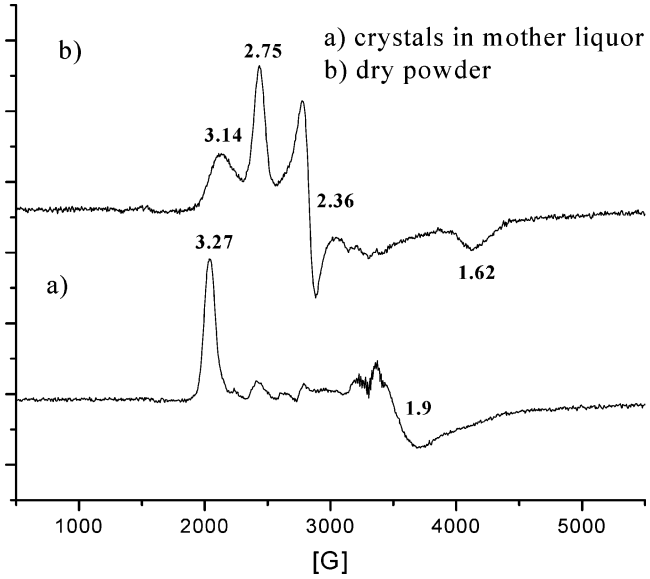

Figure 15. EPR spectrum of *perp*-$[OETPPFe(1\text{-}MeIm)_2]$-$Cl{\cdot}CHCl_3$ (a) freshly removed from the mother liquor and (b) one week later, when the crystals had decomposed to powder. Reprinted from ref 163. Copyright 2003 American Chemical Society.

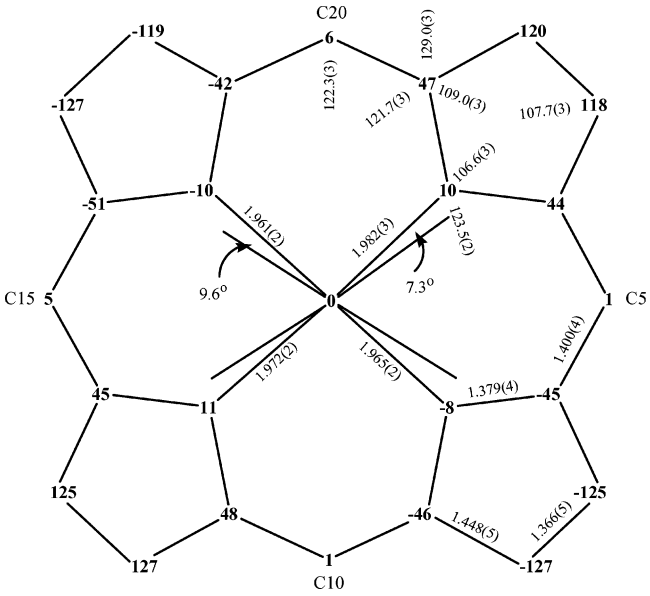

Figure 16. Formal diagram of *perp*-$[OETPPFe(1\text{-}MeIm)_2]$-$Cl{\cdot}CHCl_3$, showing the displacement of the atoms in units of 0.01 Å from the mean plane of the 25-atom core. The orientations of the axial ligands with the closest $Fe-N_P$ vector are also drawn. Reprinted from ref 163. Copyright 2003 American Chemical Society.

structure, with an axial ligand plane dihedral angle of 73.1°.[163] The molecule is nonplanar and adopts an almost purely saddled conformation with axial ligands in nearly perpendicular planes. Figure 16 displays the deviation of all atoms from the mean porphyrin plane, together with the arrangement of axial ligands.

In addition to this crystalline form of $[OETPPFe(1\text{-}MeIm)_2]^+$ with an axial ligand plane dihedral angle of 73°, a second crystalline form was also obtained. Solution of this structure also went smoothly: the refinement went well to yield an acceptable *R*-value of 0.0875,[164] which is reasonable, though not spectacular, for a metalloporphyrinate of the size of the

$[OETPPFe(1\text{-}MeIm)_2]^+$ ion. The fascinating finding in this structure was that the axial ligand plane dihedral angle, $\Delta\varphi$, was 50°, and the EPR spectrum was rhombic.[164] However, the density obtained for this *P*3(1)21 space group crystal was anomalously low, 1.064 g/cm^3,[164] as compared to the other compounds of this study, which usually have densities of about 1.3 g/cm^3.[163] The reason for the low density, based upon the structure obtained, was that there were large voids in the crystal, with a clathrate-type structure of the chloroform molecules and the chloride counterions (there is one chloroform solvate per formula unit). These clathrate-type rings, composed of six chloroform molecules and six chloride ions, persist in channels throughout the crystal.[164] We strongly suspect that the crystals of this second form, having apparent space group *P*3(1)21, are merohedral triplets, and at the time of this writing the structure has not been solved in the proper space group. The crystals readily decompose to powder upon removal of a chloroform atmosphere or the mother liquor, which would be consistent with the open clathrate-type structure of the solvate and counterion obtained provisionally for this molecule, but there is no assurance that the true axial ligand dihedral angle, $\Delta\varphi$, is 50°, or even that there is an open clathrate-type structure. The EPR spectrum obtained from this crystalline form of $[OETPPFe(1\text{-}MeIm)_2]Cl$ had a very small "large g_{max}" signal (3.16) and a much more intense normal rhombic signal (g = 2.75, 2.34, and 1.54, V/λ = 2.24, Δ/λ = 2.92, V/Δ = 0.77).[164] Other bis-ligand complexes of OETPPFe(III), including the bis-imidazole and bis-1-benzylimidazole complexes, also crystallize in the same apparent space group with the same apparently open lattice structure, and each of these sets of crystals shows a strong rhombic signal (g = 2.76, 2.35, and 1.63, V/λ = 2.40, Δ/λ = 2.95, V/Δ = 0.81; and g = 3.08, 2.19, and 1.58, V/λ = 1.76, Δ/λ = 4.47, V/Δ = 0.39, respectively); in addition, the imidazole complex also exhibits a "large g_{max}" signal at g = 3.24.[165] Observation of a strong rhombic EPR signal for all three of these complexes tells us that whatever the dihedral angle(s) between axial ligand planes actually is (are), this (these) value(s) would likely aid in narrowing the range of angles over which the changeover from a normal rhombic to a "large g_{max}" signal may occur; hence, efforts to solve these structures in the correct space group(s) are continuing.

4.2. Bis-(1-Methylimidazole) Complexes of OMTPPFe(III) and TC_6TPPFe(III): A Rich and Interesting Variety of Ligand Orientations and Core Conformations

Our continued investigations of the structures of octaalkyltetraphenylporphyrinato-iron(III) complexes have shown that these porphyrinate systems are extremely rich in structural variety. With a common axial ligand we have obtained not only the structure of *perp*-$[OETPPFe(1\text{-}MeIm)_2]Cl$ having axial ligand plane dihedral angle $\Delta\varphi$ = 73° just discussed,[163] but also two of $[OMTPPFe(1\text{-}MeIm)_2]Cl$, one (denoted *paral*-) having axial ligand plane dihedral angle $\Delta\varphi$ = 19.5°, and another of the same complex (denoted

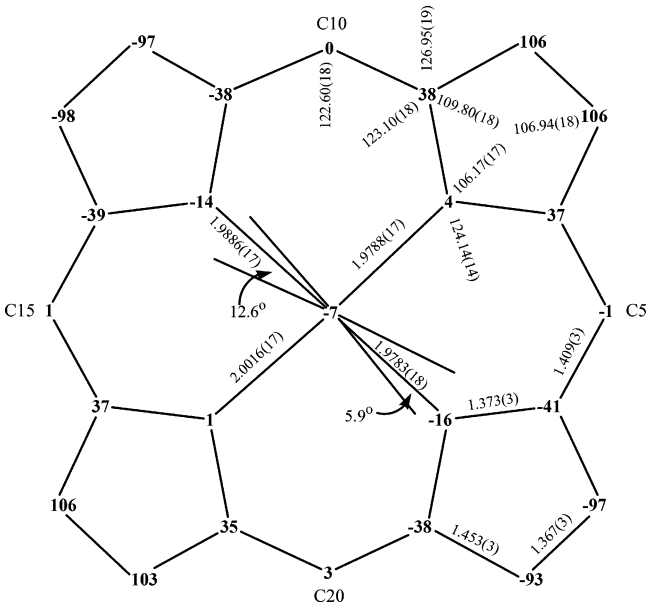

Figure 17. Formal diagram of *paral*-$[OMTPPFe(1\text{-}MeIm)_2]$-Cl showing the displacement of the atoms in units of 0.01 Å from the mean plane of the 25-atom core. The orientations of the axial ligands with the closest $Fe-N_P$ vector are also drawn. Reprinted from ref 163. Copyright 2003 American Chemical Society.

perp-) having $\Delta\varphi$ = 90°, and one of $[TC_6TPPFe(1\text{-}MeIm)_2]Cl$ having $\Delta\varphi$ = 90°; the EPR spectra of these are of the "large g_{max}" type, with g = 3.27−3.64, except for *paral*-$[OMTPPFe(1\text{-}MeIm)_2]^+$, for which a rhombic EPR signal is observed (g = 2.71, 2.53, and 1.52, V/λ = 2.44, Δ/λ = 1.87, V/Δ = 1.31).[163] The very small calculated tetragonality of 1.87 is consistent with the fact that one of the 1-MeIm ligands has a longer $Fe-N_{ax}$ bond length than the other (2.016(2) and 1.975(2) Å, respectively), thus decreasing the ligand field strength of the 1-MeIm ligand having the longer bond. A similar lowering of ligand field strength may be involved in *paral*-$[TMPFe(5\text{-}MeHIm)_2]^+$, where molecule A has different bond lengths (1.978(6) and 1.961(5) Å), while those of molecule B are much more similar (1.980(5) and 1.985(5) Å),[135] although this was not recognized at the time the work was published, and in any case, only one set of EPR parameters was observed for the crystals. The extreme lengthening of one of the $Fe-N_{ax}$ bonds in *paral*-$[OMTPPFe(1\text{-}MeIm)_2]Cl$ is much more striking.

The 19.5° dihedral angle between axial ligand planes in *paral*-$[OMTPPFe(1\text{-}MeIm)_2]Cl$, Figure 17,[163] is a very interesting feature of this structure, since saddled porphyrinates are expected to stabilize axial ligands in perpendicular planes with small angles φ_1 and φ_2. However, while the φ angles are indeed small (φ_1 = −5.9, φ_2 = 12.6°), $\Delta\varphi$ is very far from the ideal 90°. Molecular mechanics calculations on $[OETPPCo(L)_2]^+$ (L = several pyridines)[161] have shown that constraining the plane of one axial ligand to be parallel to the other gives the highest energy for the molecule (120−140 kJ/mol as compared to having the ligands in perpendicular planes).[161] (This value is expected to be considerably smaller for analogous $[OMTPPM(L)_2]^+$ complexes which are not forced to have as large a saddle distortion, and DFT calcula-

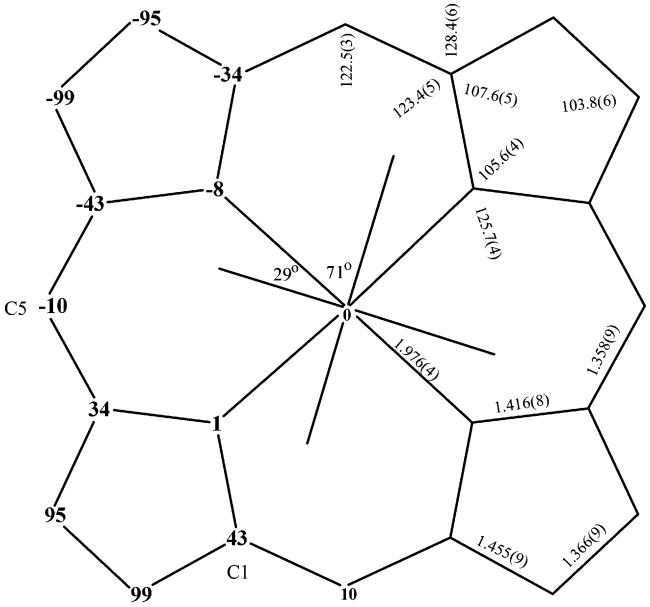

Figure 18. Formal diagram of *perp*-[OMTPPFe(1-MeIm)$_2$]-Cl showing the displacement of the atoms in units of 0.01 Å from the mean plane of the 25-atom core. The orientations of the axial ligands with the closest N_P-Fe-N_P vector are also drawn. Reprinted from ref 163. Copyright 2003 American Chemical Society.

tions on [OMTPPFe(Py)$_2$]$^+$,[163] in which the pyridine ligands were both rotated, keeping them in perpendicular planes without changing the porphyrin core conformation, yielded a maximum energy of 63 kJ/mol above the minimum. A significantly smaller maximum energy would be expected for [OMTPPFe(HIm)$_2$]$^+$.) The purely saddled structure accommodates axial ligands in nearly parallel planes by having uneven deviations of the pyrrole rings from planarity, and by having N1, N3, and Fe not in the mean porphyrin plane, but rather slightly out of it in the direction of the optimally oriented ligand (−0.15 Å for the nitrogens and −0.07 Å for Fe), as shown in Figure 17; the optimally oriented ligand is the one having $\varphi_2 = 12.6°$. In contrast, the other two nitrogens are almost in the mean plane. These adjustments, along with the two different axial ligand bond lengths, provide sufficient room for the two axial ligands along N1−N3 and the "parallel" (19.5°) orientation to be possible.[163]

perp-[OMTPPFe(1-MeIm)$_2$]Cl also has unique structural features, for although the axial ligands are in perfectly perpendicular planes, the angle between the N_P-Fe-N_P axes, $\varphi = 29°$, is considerably larger than considered optimal on the basis of molecular mechanics calculations.[161] This large φ angle is made possible by the less severe steric requirements of the five-membered imidazole ring, and some ruffling of this mainly saddled porphyrinate complex, as shown in Figure 18. The positions of two adjacent β-carbons are alternantly displaced by ±0.95 and ±0.99 Å from the 25-atom mean plane, and the *meso*-carbons lie ±0.10 Å out of this plane.[163] The similarity in the core conformations of the three bis-(1-MeIm) complexes discussed thus far is made evident by the plot of the linear deviations of the core atoms from the mean plane of *perp*-[OETPPFe(1-MeIm)$_2$]Cl (blue), *paral*-[OMTPPFe(1-MeIm)$_2$]Cl (black), and *perp*-[OMTPPFe(1-MeIm)$_2$]Cl (red) shown in Figure 19 (top).

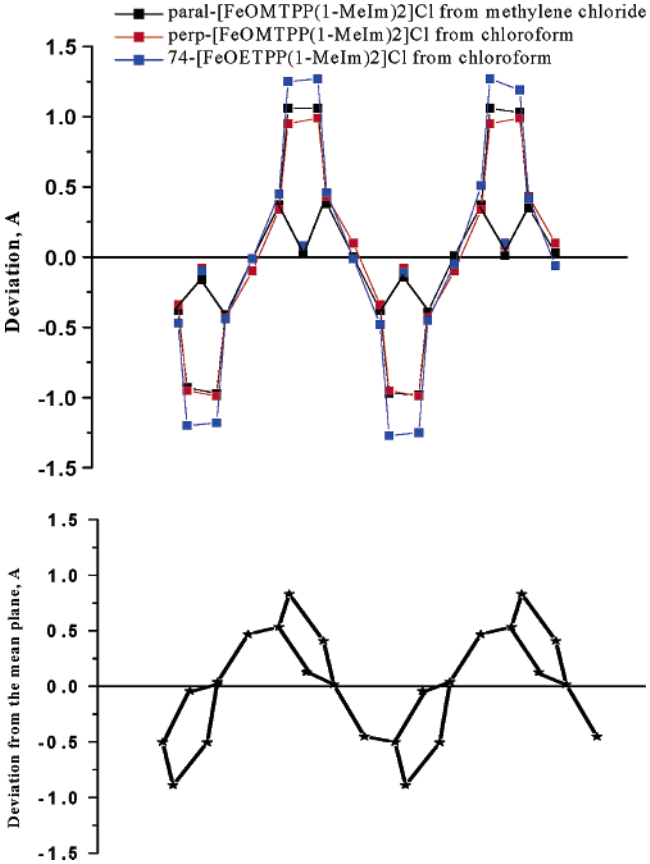

Figure 19. Plot of the linear deviations of the core atoms from the mean plane (top) for (blue) *perp*-[OETPPFe(1-MeIm)$_2$]$^+$, (black) *paral*-[OMTPPFe(1-MeIm)$_2$]$^+$, and (red) *perp*-[OMTPPFe(1-MeIm)$_2$]$^+$, and (bottom) for [TC$_6$TPPFe-(1-MeIm)$_2$]$^+$. Reprinted from ref 163. Copyright 2003 American Chemical Society.

The structure of [TC$_6$TPPFe(1-MeIm)$_2$]Cl also has the axial ligands in exactly perpendicular planes, as shown in Figure 20, but in this case with a much smaller angle $\varphi = 15.3°$. In spite of the smaller φ angle than for *perp*-[OMTPPFe(1-MeIm)$_2$]Cl, this molecule is the most ruffled of the saddled iron(III) porphyrinates of this study, with the *meso*-carbons out of the 25-atom mean plane by ±0.26 Å.[163] This complex is also the least saddled of the complexes studied. The plot of the linear deviations of the core atoms from the mean plane of this molecule is entirely different from that shown in Figure 19 (top), and is shown in Figure 19 (bottom). The angle of minimum energy between the projection of the axial ligand plane and the closest N_P-Fe-N_P vector for [OETPPCo(1-MeIm)$_2$]$^+$ (saddled) and [T^{t}BuPCo(1-MeIm)$_2$]$^+$ (ruffled) is 2−3° for the saddled and 45° for the ruffled conformation for five-membered aromatic sterically non-hindered axial ligands.[161] The 15.3° angle found for [TC$_6$TPPFe(1-MeIm)$_2$]$^+$ is reasonably close to that calculated (about 4° smaller) for the admixture of saddled and ruffled conformations of the porphyrin core.[163]

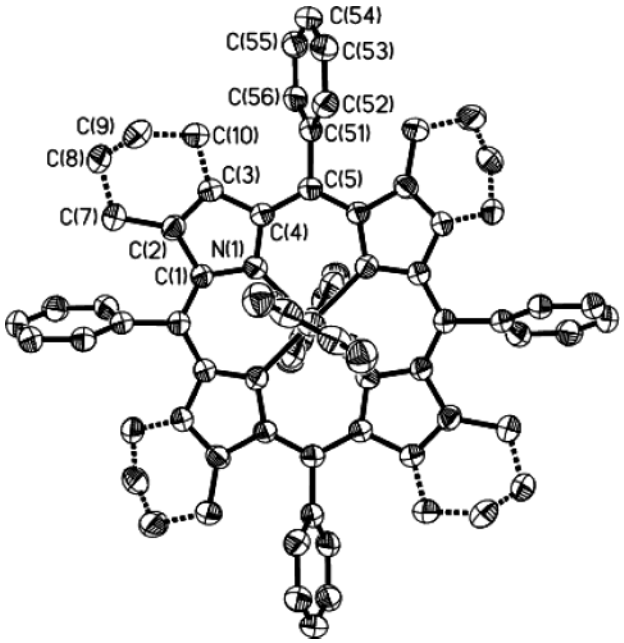

Figure 20. ORTEP diagram of the porphyrin macrocycle of $[TC_6TPPFe(1\text{-}MeIm)_2]Cl$. Thermal ellipsoids are shown at 50% probability. Perpendicular orientation of the axial ligands can clearly be seen. Hydrogen atoms have been omitted for clarity. Reprinted from ref 163. Copyright 2003 American Chemical Society.

4.3. The Bis-(4-Dimethylaminopyridine) and -(2-Methylimidazole) Complexes of OMTPPFe(III)

An additional four complexes have also been prepared and characterized by X-ray crystallography and EPR spectroscopy, two of $[OMTPPFe(4\text{-}NMe_2\text{-}Py)_2]Cl$ (denoted A and B), having $\Delta\varphi = 79°$ ($\varphi_1 = -0.8°$, $\varphi_2 = 78°$, highly saddled and ruffled with $|\Delta C_m| = \pm 0.35$ Å) and 89° ($\varphi_1 = -1.0°$, $\varphi_2 = 87.5°$, nearly purely saddled with $|\Delta C_m| = \pm 0.07$ Å), respectively, and two of $[OMTPPFe(2\text{-}MeHIm)_2]Cl$ (denoted C and D), having $\Delta\varphi = 81°$ ($\varphi_1 = -11.2°$, $\varphi_2 = 69.5°$, saddled and somewhat ruffled with $|\Delta C_m| = 0.13$ Å) and 84° ($\varphi_1 = -13.1°$, $\varphi_2 = 71.0°$, saddled and more ruffled with $|\Delta C_m| = 0.21$ Å), respectively.[163] The frozen solution EPR spectra of these complexes have g_{max} values at 3.29 and 3.27, respectively.

The three pairs of structures of low-spin Fe(III) complexes of OMTPP presented in this work[163] show the diversity of ligand binding capabilities exhibited in this system and the richness of the information obtained therefrom.

4.4. Summary of EPR and Mössbauer Spectroscopic Results for OETPPFe(III) and OMTPPFe(III) Complexes

The EPR data for representative complexes having "parallel" and "perpendicular" orientations of the ligand planes are summarized in Table 2, where it can be seen that the calculated tetragonalities (Δ/λ) for bis-imidazole and -4-dimethylaminopyridine complexes are generally in the range of 2.8−3.5, as found previously for the B hemichromes (Figure 1), with a few notable exceptions: First, the small value observed for *paral*-$[OMTPPFe(1\text{-}MeIm)_2]^+$, $\Delta/\lambda = 1.82$, Table 2, is likely due to the long bond of one of the imidazole ligands,[163] as mentioned earlier in this review. *perp*-$[OMTPPFe(1\text{-}MeIm)_2]^+$ shows a somewhat larger value of the tetragonality (Table 2, $\Delta/\lambda = 3.93$). In this latter case, since the two smaller *g*-values were determined from the magnetic Mössbauer spectra,[166] there is some possibility of error in the values determined, because the Mössbauer spectral fits are much less sensitive to the values of the two smaller hyperfine coupling constants than they are to the largest value.[82,85] For the crystalline sample of $[OETPPFe(1\text{-}MeIm)_2]Cl$, with a 73° dihedral angle between axial ligand planes, listed as *perp*-$[OETPPFe(1\text{-}MeIm)_2]^+$ in Table 2, for which two *g*-values appear to be resolved (Figure 15), $\Delta/\lambda = 5.09$, a value previously thought to be typical of the axial ligand set imidazole−hydroxide[68,69] and later shown to also be consistent with two imidazolate ligands (Table 2, $\Delta/\lambda = 4.94$).[120] However, because 1-MeIm cannot be deprotonated, this unreasonable value suggests that the second feature observed in the EPR spectrum of these crystals is not indicative of the second *g*-value, but instead results from preferential orientations of the crystallites. (The EPR sample tube should have been rotated to test this hypothesis.) Indeed, the Mössbauer spectral fits are consistent with *g*-values of 3.27, 2.00, and 1.14,[166] yielding a value of $\Delta/\lambda = 3.44$ and $V/\Delta = 0.36$. Therefore, the second feature in the EPR spectrum of *perp*-$[OETPPFe(1\text{-}MeIm)_2]^+$ (Figure 15) must indeed result from preferential orientations of the crystallites and should not be taken seriously; thus only the Mössbauer-derived value is included in Table 2. Thus, for these "large g_{max}" complexes, only the maximum *g*-value can be measured by EPR spectroscopy, while the other two *g*-values are best measured by single-crystal EPR or estimated by magnetic Mössbauer spectroscopy. As for the rhombicities, for all Type II complexes $V/\Delta = 0.49$ or larger, while for all Type I complexes $V/\Delta = 0.36$ or smaller, and even for complexes having axial ligands in perfectly perpendicular planes there is some Jahn−Teller distortion that yields a rhombic component to the d-orbital energy diagram, albeit smaller than for the complexes having axial ligands in parallel planes.

As indicated in the preceding paragraph, detailed Mössbauer spectroscopic investigations of four of the crystalline octaalkyltetraphenylporphyrinatoiron(III) complexes, *paral*-$[OMTPPFe(1\text{-}MeIm)_2]Cl$, *perp*-$[OETPPFe(4\text{-}NMe_2Py)_2]Cl$, *perp*-$[OETPPFe(1\text{-}MeIm)_2]Cl$, and *perp*-$[OMTPPFe(1\text{-}MeIm)_2]Cl$, having axial ligand dihedral angles of 19.5, 70, 73,, and 90°, respectively, have been carried out.[166] The spectra of these crystalline samples, that were frozen immediately after removal from the mother liquor and transfer to the Mössbauer sample holder, were much easier to fit than those of powdered solid or frozen glassy samples studied previously,[85] probably because of the fact that all molecules in the sample have the same axial ligand plane orientations; no signals due to impurities were detected. The data obtained are listed in Table 4, along with magnetic Mössbauer data from other model heme complexes discussed in this review. As can be seen, the "parallel" complex has a much larger quadrupole splitting than do any

Table 4. Mössbauer Data for Model Heme Complexes Discussed in This Work

system	δ, mm/s	ΔE_Q, mm/s	η	$A_{xx}/g_N\mu_N$, kG	$A_{yy}/g_N\mu_N$, kG	$A_{zz}/g_N\mu_N$, kG	ref
$[TPPFe(2\text{-}MeHIm)_2]^+$ [a]	0.21	1.71	−2.0	−347	220	810	82
$[TMPFe(4\text{-}NMe_2Py)_2]^+$		1.75	−1.0	−331	168	815	87
perp-$[OMTPPFe(1\text{-}MeIm)_2]^+$	0.27	1.76	−0.99	−229	294	901	166
perp-$[OETPPFe(1\text{-}MeIm)_2]^+$	0.21	1.94	−0.94	−376	235	714	166
perp-$[OETPPFe(4\text{-}NMe_2Py)_2]^+$	0.21	1.89	−0.43	−366	51	718	166
paral-$[OMTPPFe(1\text{-}MeIm)_2]^+$	0.27	2.80	−0.36	−422	236	502	166
$[OEPFe(4\text{-}NMe_2Py)_2]^+$		2.15	−1.8	−416	177	446	87
$[OEPFe(1\text{-}MeIm)_2]^+$ [b]	0.26	2.28	−1.8	−330	30	550	170

[a] Frozen solution sample. Solvent = dimethylformamide. [b] Frozen solution sample. Solvent = dimethylacetamide.

of the three "perpendicular" complexes. This result is consistent with previous studies,[82,85,87] and is expected because the "parallel" complex, with large rhombicity, should have a much more asymmetric electron distribution than do the "perpendicular" complexes. The isomer shifts of the four complexes are within close to experimental error of each other, as is expected for low-spin Fe(III) complexes. The hyperfine coupling constants of the complexes are also consistent with those reported previously,[82,85,87] with the largest-magnitude hyperfine coupling constant, A_{zz}, being considerably smaller for the "parallel" complex (502 kG) than for the strictly perpendicular complex (901 kG), A_{xx} being negative for all four complexes and largest in magnitude for the "parallel" complex (−422 kG) and smallest in magnitude for the strictly perpendicular complex (−229 kG), and A_{yy} being small and positive, but difficult to estimate with accuracy for all four complexes. As shown previously,[85] there are direct correlations between A_{zz} and A_{xx}, between g_{zz} and A_{zz} (in fact, A_{zz} can be estimated from the overall spread of the magnetic Mössbauer spectrum, as well as from the value of g_{zz}[82,85]), and between V/Δ and A_{zz} for these four complexes. There is also a rough correlation between the axial ligand plane dihedral angle $\Delta\varphi$ and the value of A_{zz}.[166] Thus, these complexes, like other $(d_{xy})^2(d_{xz},d_{yz})^3$ ground-state systems,[85] exhibit a continuum of decreasing A_{zz} values that exist for Type I and Type II complexes. The *perp*-[OMTPPFe(1-MeIm)$_2$]Cl complex has a value of A_{zz} that is among the largest reported thus far,[85] with only cytochrome b_6,[167] heme *c* of *Thiobacillus denitrificans* cytochrome cd_1 nitrite reductase,[168] and low-spin heme *c* (1) of *Desulfovibrio desulfuricans* hexaheme nitrite reductase[169] (926, 910, and 926 kG, respectively) having slightly larger values, and *paral*-[OMTPPFe(1-MeIm)$_2$]Cl has a value of A_{zz} that is typical of complexes known to have axial ligands in strictly or at least nearly parallel planes, including $[OEPFe(4\text{-}NMe_2Py)_2]ClO_4$,[87] $[OEPFe(1\text{-}MeIm)_2]ClO_4$,[170] $[((OMe)_2)_4TPPFe(1\text{-}MeIm)_2]^+$,[85] and $[((OMe)_2)_4TPPFe(4\text{-}NMe_2Py)_2]^+$ [85] among model hemes (446, 550, 530, and 500 kG, respectively) and low-spin hemes *c* (4) and (5) of *D. desulfuricans* hexaheme nitrite reductase[169] (540 and 505 kG, respectively) among heme proteins. Although it would, in principle, be interesting to carry out a magnetic Mössbauer spectroscopic investigation of mitochondrial Complex III, the cytochrome bc_1 complex, the presence of three heme centers, all with "large g_{max}" EPR signals,[77] would make deconvolution of the three overlapping spectra with likely similar values of A_{zz} extremely difficult, unless redox titrations were to be carried out, as in the case of the EPR spectra of Complex III shown in Figure 2.[76,77]

5. Conclusions

From investigations of synthetic low-spin ferriheme model complexes it has been found that for those in which the axial ligands are in "perpendicular" planes, "large g_{max}" EPR signals are observed when the dihedral angle between ligand planes, $\Delta\varphi$, is as small as 70°,[162,163] while normal rhombic EPR signals are observed when the dihedral angle is as large as 30°.[135] Thus, the switch in EPR signal type from normal rhombic (Type II)[84] to "large g_{max}" (Type I)[84] must occur at a dihedral angle somewhere between 30° and 70°. These findings narrow the range of angles over which the type of EPR signal must switch from normal rhombic to "large g_{max}", and they significantly modify our understanding of what "perpendicular" may actually mean in the structures of the bis-histidine-coordinated cytochromes of mitochondrial Complexes II and III. Although it is possible that heme b_H of the bc_1 complex, with "large g_{max}" signal at $g = 3.41-3.44$,[77] does have an imidazole plane dihedral angle as small as the 38° used for model building for the present stage of refinement,[88] such a small angle seems unlikely on the basis of the results presented herein. Furthermore, with regard to off-axis tilting of the axial ligands, there appears to be no clear evidence from model heme studies reported to the present that the EPR spectrum is influenced by such tilting; in Table 2 it is seen that the largest off-axis tilts of the axial ligands, for *perp*-$[TMPFe(5\text{-}MeHIm)_2]^+$, $\sum$tilts = 20.1° with a dihedral angle $\Delta\phi = 76°$,[135] has a smaller *g*-value than does *perp*-$[OETPPFe(1\text{-}MeIm)_2]^+$ (3.12 as compared to 3.27), which has a much smaller $\sum$tilts = 5.8° with a dihedral angle $\Delta\phi = 73°$,[163] while $[TC_6TPPFe(1\text{-}MeIm)_2]^+$ has the largest *g*-value (3.64), strictly perpendicular ligand planes ($\Delta\phi = 90°$), and no tilting of axial ligands ($\sum$tilts = 0°).[163] Furthermore, *paral*-$[TMPFe(5\text{-}MeHIm)_2]^+$, for which there are two molecules in the unit cell, with ligand plane dihedral angles $\Delta\phi = 26$ and 30° and off-axis $\sum$tilts = 5.7 and 10.2°, shows such similar EPR spectra that they cannot be deconvoluted.[135] The EPR signal observed for the *perp*-$[OETPPFe(1\text{-}MeIm)_2]Cl$ complex having the 73° dihedral angle has a smaller *g*-value (3.27)[163] than that observed for the bc_1 heme b_H,[77] and the *g*-value of heme b_H is identical to that of $[TPPFe(2\text{-}MeHIm)_2]^+$ (3.41),[82] where the dihedral

angle is 89°.[83] (It is hoped that saddling of the porphyrinate ring does not itself affect the value of g_{max} or the axial ligand plane dihedral angle at which the EPR signal type switches from Type I to Type II, but further investigations will be necessary in order to clarify this point. At least, the similarity in the values for *paral*-$[OMTPPFe(1\text{-}MeIm)_2]^+$ and $[TC_6TPPFe(1\text{-}MeIm)_2]^+$ (g = 3.61, 3.64) despite the differences in core conformation (Figure 19), and the similarity (and smaller magnitude) for the g_{max} values of $[OETPPFe(4\text{-}Me_2NPy)_2]^+$ and $[OETPPFe(1\text{-}MeIm)_2]^+$ (70, 73°, g = 3.29−3.35, 3.27[163]) is encouraging.) All of the data for model heme complexes of known axial ligand dihedral angles have been scrutinized carefully, and although there is a very rough correlation between axial ligand dihedral angle and the value of g_{max} for the non-N−H imidazole complexes that would predict that the switchover to a normal rhombic EPR signal may occur at a dihedral angle somewhere between 50° and 60° (not a shocking suggestion), there is no structural basis for excluding N−H imidazoles, for both structures (of $[TPPFe(2\text{-}MeHIm)_2]^+$ [83] and *perp*-$[TMPFe(5\text{-}MeHIm)_2]^+$ [135]) show no significant interactions of the N−H groups with anything except the perchlorate anion, a very weak base that should not perturb the ligand field strength of the imidazole significantly. Thus, we can find no clear correlation between structural features (bond lengths, axial ligand plane dihedral angles, out-of-plane distortions of porphyrin nitrogens, or even tilting of axial ligands from the heme normal) and the "large g_{max}" value. Furthermore, we have no structurally characterized model complexes with "large g_{max}" values as large as that of heme b_L (3.71−3.79),[77] nor do we have an idea how to create such a large g-value in a bis-imidazole-coordinated ferriheme. Among all axial ligands, only bis-cyanide complexes have "large g_{max}" values similar to this (3.75).[171]

Although saddled Fe(III) porphyrinates have been used for the latest attempts to model the bis-histidine-ligated cytochromes,[162,163] it is not proposed that the membrane-bound proteins have highly saddled hemes. Rather, these Fe(III) octaalkyltetraphenylporphyrinates have been used because they allow the possibility, in model heme complexes that are unconstrained with respect to their surroundings (in contrast to the heme centers in membrane-bound proteins), for axial ligands to lie close to the N_P-Fe-N_P axes in perpendicular planes, which may stabilize Fe(II) complexes with this axial ligand arrangement. It remains to be seen whether this will in fact be the case; attempts to prepare crystalline samples of the Fe(II) analogues of several of the Fe(III) complexes of the present study are in progress. What has been found in the most recent work[163] is that the Fe(III) octaalkyltetraphenylporphyrinates provide a rich variety of axial ligand orientations and porphyrin core conformations, among which are several that lead to important insights into the possibilities for axial ligand orientations in the membrane-bound heme proteins.

6. Acknowledgments

The support of the National Institutes of Health, grant DK31038, over the years of this project is gratefully acknowledged. Many collaborators, coworkers, and students have contributed significantly to the work reported from this laboratory that is referenced herein. First and foremost, Professor W. R. Scheidt of the University of Notre Dame and his student, Dr. Martin Safo, carried out the large number of structural determinations that have led to the understanding of the tetramesitylporphyrinatoiron(III) and -(II) complexes. In this work, as well as that on other synthetic iron(III) and -(II) porphyrinates, Mössbauer spectroscopy has played an important role in understanding the magnetic properties of these centers, and it has been vital to estimating the two unresolved g-values of the Fe(III) porphyrinates that have "large g_{max}" EPR spectra, and to obtaining a complete understanding of the magnetic properties of these complexes. In order of their involvement in this work, the scientists who have carried out these studies are Professor B. H. (Vincent) Huynh of Emory University, Dr. Govind Gupta, then of Penn State University, Professor Peter Debrunner of the University of Illinois, and Professor Alfred X. Trautwein and Dr. Volker Schünemann of the University of Lübeck. Graduate students involved in this work include Ms. Mabry Benson, Dr. Marlys J. M. Nesset, Dr. C. Todd Watson, Dr. Konstantin I. Momot, Dr. Sheng Cai, Dr. Hiroshi Ogura, and Dr. Liliya A. Yatsunyk, who herself has solved over 20 molecular structures by X-ray crystallography during her Ph.D. studies. Postdoctoral associates Dr. Gloria B. Merrill and Dr. Robert S. McLeod synthesized the six-coordinate TPPFe(III) complexes with imidazole ligands covalently attached to adjacent (cis) and opposite (trans) phenyl rings. Senior research scientists Dr. Andrei V. Astashkin (pulsed EPR spectroscopy), Dr. Tatjana Kh. Shokhireva (NMR spectroscopy), and Dr. Nikolai V. Shokhirev (computer software for data analysis) have contributed extensively to this work, and Dr. Arnold M. Raitsimring (EPR Facility Head), Dr. Michael D. Carducci (Molecular Structure Facility Head), and Dr. Neil E. Jacobsen (NMR Facility Head) have provided vital expertise and support to graduate students, senior research scientists, and the author. Editorial assistant Mary T. Flores provided exceptionally important help in the preparation of the figures. This review is dedicated to the memory of Professor Richard Koerner of Pennsylvania State University, who, as an undergraduate researcher in the author's laboratory for three years (her first student at Arizona), carried out an extensive study of unsymmetrically substituted derivatives of TPPFe(III) that led to our understanding of the effects of *ortho*-phenyl substituents on the electronic properties of these complexes.

7. Abbreviations

EPR	electron paramagnetic resonance
NMR	nuclear magnetic resonance
TPP	tetraphenylporphyrin
OEP	octaethylporphyrin

TMP	*meso*-tetramesitylporphyrin
2,6-Cl_2TPP	*meso*-tetra-(2,6-dichlorophenyl)porphyrin
Proto IX	protoporphyrin IX
OETPP	octaethyltetraphenylporphyrin
OMTPP	octamethyltetraphenylporphyrin
TC_6TPP	tetra-(3,4-tetramethylene)-tetraphenylporphyrin
T^nPrP	*meso*-tetra-*n*-propylporphyrin
T^iPrP	*meso*-tetra-isopropylporphyrin
T^tBuP	*meso*-tetra-*tert*-butylporphyrin
K222	cryptate ligand for potassium ion (4,7,13,16,-21,24-hexaoxa-1,10-diazabicyclo[8.8.8]-hexacosane)
2-MeHIm	2-methylimidazole
HIm	imidazole
1-MeIm	1-methylimidazole
1-VinIm	1-vinylimidazole
1-Me_3SiIm	1-trimethylsilylimidazole
1,2-Me_2Im	1,2-dimethylimidazole
5-MeHIm	5-methylimidazole
4-NMe_2Py	4-dimethylaminopyridine
4-NH_2Py	4-aminopyridine
3-MePy	3-methylpyridine
3-EtPy	3-ethylpyridine
Py	pyridine
3-ClPy	3-chloropyridine
3-CNPy	3-cyanopyridine
4-CNPy	4-cyanopyridine
NOESY	nuclear Overhauser and exchange spectroscopy
EXSY	exchange spectroscopy
DFT	density functional theory
paral-	axial ligands in approximately parallel planes
perp-	axial ligands in approximately perpendicular planes

8. References

(1) Margoliash, E.; Schejter, A. *Trends Biochem. Sci.* **1984**, *9*, 364.
(2) Keilin, D. *Proc. R. Soc. London B: Biol. Sci.* **1925**, *98*, 312.
(3) Slater, E. C. *J. Biol. Chem.* **2003**, *278*, 16455.
(4) *Cytochrome P450: Structure, Mechanism and Biochemistry*, 2nd ed.; Ortiz de Montellano, P. R., Ed.; Plenum: New York, 1995.
(5) See http://drnelson.utmem.edu/nelsonhomepage.html and http://p450.antibes.inra.fr/ for recent compilations of P450 genes and their sequences.
(6) Mao, J.; Hauser, K.; Gunner, M. R. *Biochemistry* ***2003***, *42*, 9839.
(7) La Mar, G. N.; Jackson, J. T.; Dugad, L. B.; Cusanovich, M. A.; Bartsch, R. G. *J. Biol. Chem.* **1990**, *265*, 16173.
(8) Bertini, I.; Gori, G.; Luchinat, C.; Vila, A. J. *Biochemistry* **1993**, *32*, 776.
(9) Clark, K.; Dugad, L. B.; Bartsch, R. G.; Cusanovich, M. A.; La Mar, G. N. *J. Am. Chem. Soc.* **1996**, *118*, 4654.
(10) Finzel, B. C.; Weber, P. C.; Hardman, K. D.; Salemme, F. R. *J. Mol. Biol.* **1985**, *186*, 627.
(11) Yasui, M.; Harada, S.; Kai, Y.; Kasai, N.; Kusonoki, M.; Matsuura, Y. *J. Biochem.* **1992**, *111*, 317.
(12) Ren, Z.; Meyer, T.; McRee, D. E. *J. Mol. Biol.* **1993**, *234*, 433.
(13) Archer, M.; Banci, L.; Dikaya, E.; Romão, M. J. *J. Biol. Inorg. Chem.* **1997**, *2*, 611.
(14) Tahirov, T. H.; Misaki, S.; Meyer, T. E.; Cusanovich, M. A.; Higuchi, Y.; Yasuoka, N. *J. Mol. Biol.* **1996**, *259*, 467.
(15) Dobbs, A. J.; Anderson, B. F.; Faber, H. R.; Baker, E. N. *Acta Crystallogr.* **1996**, *D52*, 356.
(16) Shibata, N.; Iba, S.; Misaki, S.; Meyer, T. E.; Bartsch, R. G.; Cusanovich, M. A.; Morimoto, Y.; Higuchi, Y.; Yasuoka, N. *J. Mol. Biol.* **1998**, *284*, 751.
(17) Widger, W. R.; Cramer, W. A.; Herrmann, R. G.; Trebst, A. *Proc. Natl. Acad. Sci. U.S.A.* **1984**, *81*, 674.
(18) von Jagow, G.; Engel, W. D. *Angew. Chem., Int. Ed. Engl.* **1980**, *19*, 659.
(19) Ohnishi, T.; Schagger, H.; Meinhardt, S. W.; LoBrutto, R.; Link, T. A.; von Jagow, G. *J. Biol. Chem.* **1989**, *264*, 735.
(20) Daldar, F.; Tokito, M. K.; Davidson, E.; Faham, M. *EMBO J.* **1989**, *8*, 3951.
(21) Xia, D.; Yu, C.-A.; Kim, H.; Xia, J.-Z.; Kachurin, A. M.; Zhang, L.; Yu, L.; Deisenhofer, J. *Science* **1997**, *277*, 60.
(22) Iwata, S.; Lee, J. W.; Okada, K.; Lee, J. K.; Iwata, M.; Rasmussen, B.; Link, T. A.; Ramaswamy, S.; Jap, B. K. *Science* **1998**, *281*, 64.
(23) Zhang, Z.; Huang, L.; Shulmeister, V. M.; Chi, Y.-I.; Kim, K. K.; Hung, L.-W.; Crofts, A. R.; Berry, E. A.; Kim, S.-H. *Nature* **1998**, *392*, 677.
(24) T'sai, A.-L.; Palmer, G. *Biochim. Biophys. Acta* **1983**, *722*, 349.
(25) Hunte, C.; Koepke, J.; Lange, C.; Rossmanith, T.; Michel, H. *Structure* **2000**, *8*, 669.
(26) Yang, X.; Trumpower, B. L. *J. Biol. Chem.* **1988**, *263*, 11962.
(27) Schütz, M.; Schoepp-Cothenet, B.; Lojou, E.; Woodstra, M.; Lexa, D.; Tron, P.; Dolla, A.; Durand, M.-C.; Stetter, K. O.; Baymann, F. *Biochemistry* **2003**, *42*, 10800.
(28) Gabellini, N.; Hauska, G. *FEBS Lett.* **1983**, *154*, 171.
(29) Takamiya, K.; Obata, S. *Biochim. Biophys. Acta* **1986**, *852*, 198.
(30) Hobbs, D. D.; Kriauciunas, A.; Güner, S.; Knaff, D. B.; Ondrias, M. R. *Biochim. Biophys. Acta* **1990**, *1018*, 47.
(31) Breyton, C. *Biochim. Biophys. Acta* **2000**, *1459*, 467.
(32) Salerno, J. C.; McGill, J. W.; Gerstle, G. C. *FEBS Lett.* **1983**, *162*, 257.
(33) Furbacher, P. N.; Girvin, M. E.; Cramer, W. A. *Biochemistry* **1989**, *28*, 8990.
(34) Mathews, F. S.; Czerwinski, E. W.; Argos, P. In *The Porphyrins*; Dolphin, D., Ed; Academic Press: New York, 1979; Vol. VII, p 108.
(35) Lederer, F.; Ghrir, R.; Guiard, B.; Cortial, S.; Ito, A. *Eur. J. Biochem.* **1983**, *132*, 95.
(36) Douglas, R. H.; Hultquist, D. E. *Proc. Natl. Acad. Sci. U.S.A.* **1978**, *75*, 3118.
(37) Kipke, C. A.; Cusanovich, M. A.; Tollin, G.; Sunde, R. A.; Enemark, J. H. *Biochemistry* **1988**, *27*, 2918.
(38) Lui, S. M.; Soriano, A.; Cowan, J. A. *Biochem. J.* **1994**, *304*, 441.
(39) *Fourty-Second Symposium of the Society for General Microbiology: The Nitrogen and Sulphur Cycles*; Cole, J. A., Ferguson, S. J., Eds.; Cambridge University Press: Cambridge, 1988.
(40) Crane, B. R.; Siegel, L. M.; Getzoff, E. D. *Science* **1995**, *270*, 59.
(41) Huynh, B. H.; Lui, M. C.; Moura, J. J. G.; Moura, I.; Ljungdahl, P. O.; Münck, E.; Payne, W. J.; Peck, H. D.; DerVartanian, D. V.; LeGall, J. *J. Biol. Chem.* **1982**, *257*, 9576.
(42) *Molecular and Genetic Aspects of Nitrate Asimilation*; Wray, J. L., Kinghorn, J. R., Eds.; Oxford Science Publications: Oxford, 1989.
(43) Averill, B. A. *Chem. Rev.* **1996**, *96*, 2951.
(44) Jafferji, A.; Allen, J. W. A.; Ferguson, J. J.; Fülöp, V. *J. Biol. Chem.* **2000**, *275*, 25089.
(45) Einsle, O.; Messerschmidt, A.; Stach, P.; Bourenkov, G. P.; Bartunik, H. D.; Huber, R.; Kroneck, P. M. H. *Nature* **1999**, *400*, 476.
(46) Einsle, O.; Stach, P.; Messerschmidt, A.; Simon, J.; Kröger, A.; Huber, R.; Kroneck, P. M. H. *J. Biol. Chem.* **2000**, *275*, 39608.
(47) Xia, Z.-X.; Shamala, N.; Bethge, P. H.; Lim, L. W.; Bellamy, H. D.; Xuong, N. H.; Lederer, F.; Mathews, F. S. *Proc. Natl. Acad. Sci. U.S.A.* **1987**, *84*, 2629.
(48) Dubois, J.; Chapman, S. K.; Mathews, F. S.; Reid, G. A.; Lederer, F. *Biochemistry* **1990**, *29*, 6393.
(49) Yankovskaya, V.; Horsefield, R.; Törnroth, S.; Luna-Chavez, C.; Miyoshi, H.; Léger, C.; Byrne, B.; Cecchini, G.; Iwata, S. *Science* **2003**, *299*, 700.
(50) Iverson, T. M.; Luna-Chavez, C.; Cecchini, G.; Rees, D. C. *Science* **1999**, *284*, 1961.
(51) Lancaster, C. R. D. *Biochim. Biophys. Acta* **2002**, *1553*, 1.
(52) Lemos, R. S.; Fernandes, A. S.; Pereira, M. M.; Gomes, C. M.; Teixeira, M. *Biochim. Biophys. Acta* **2002**, *1553*, 158.
(53) Lancaster, C. R. D.; Kröger, A.; Auer, M.; Michel, H. *Nature* **1999**, *402*, 377.
(54) Jormakka, M.; Törnroth, S.; Byrne, B.; Iwata, S. *Science* **2002**, *295*, 1863.
(55) Pierrot, M.; Haser, R.; Frey, M.; Payan, F.; Astier, J.-P. *J. Biol. Chem.* **1982**, *257*, 14341.
(56) Higuchi, Y.; Kusunoki, M.; Matsuura, Y.; Yasuoka, N.; Kakudo, M. *J. Mol. Biol.* **1984**, *172*, 109.
(57) Ma, J.-G.; Zhang, J.; Franco, R.; Jia, S.-L.; Moura, I.; Moura, J. J. G.; Kroneck, P. M. H.; Shelnutt, J. A. *Biochemistry* **1998**, *37*, 12431.
(58) Simões, P.; Matias, P. M.; Morais, J.; Wilson, K.; Dauter, Z.; Carrondo, M. A. *Inorg. Chim. Acta* **1998**, *273*, 213.
(59) Nørager, S.; Legrand, P.; Pieulle, L.; Hatchikian, C.; Roth, M. *J. Mol. Biol.* **1999**, *290*, 881.
(60) Babcock, G. T.; Widger, W. R.; Cramer, W. A.; Oertling, W. A.; Metz, J. *Biochemistry* **1985**, *24*, 3638.
(61) Stewart, D. H.; Brudvig, G. W. *Biochim. Biophys. Acta* **1998**, *1367*, 63.
(62) Kaminskaya, O.; Kurreck, J.; Irrgang, K.-D.; Renger, G.; Shuvalov, V. A. *Biochemistry* **1999**, *38*, 16223.
(63) Kisker, C.; Schindelin, H.; Pacheco, A.; Wehbi, W.; Garrett, R. M.; Rajagopalan, K. V.; Enemark, J. H.; Rees, D. C. *Cell* **1997**, *91*, 973.
(64) Thompson, L. K.; Miller, A.-F.; Buser, C. A.; de Paula, J. C.; Brudvig, G. W. *Biochemistry* **1989**, *28*, 8048.

(65) Roncel, M.; Boussac, A.; Zurita, J. L.; Bottin, H.; Sugiura, M.; Kirilovsky, D.; Ortega, J. M. *J. Biol. Inorg. Chem.* **2003**, *8*, 206.
(66) Benosman, H.; Asso, M.; Bertrand, P.; Yagi, T.; Gayda, J.-P. *Eur J. Biochem.* **1989**, *182*, 51.
(67) Park, J.-S.; Ohmura, T.; Kano, K.; Sagara, T.; Niki, K.; Kyogoku, Y.; Akutsu, H. *Biochim. Biophys. Acta* **1996**, *1293*, 45.
(68) Blumberg, W. E.; Peisach, J. *Adv. Chem. Ser.* **1971**, *100*, 271.
(69) Peisach, J.; Blumberg, W. E.; Adler, A. D. *Ann. N.Y. Acad. Sci.* **1973**, *206*, 310.
(70) Taylor, C. P. S. *Biochim. Biophys. Acta* **1977**, *491*, 137.
(71) Palmer, G. *Biochem. Soc. Trans.* **1985**, *13*, 548.
(72) Muhoberac, B. B.; Wharton, D. C. *J. Biol. Chem.* **1983**, *258*, 3019.
(73) Brautigan, D. L.; Feinberg, B. A.; Hoffman, B. M.; Margoliash, E.; Peisach, J.; Blumberg, W. E. *J. Biol. Chem.* **1977**, *252*, 574.
(74) Orme-Johnson, N. R.; Hansen, R. E.; Beinert, H. *Biochem. Biophys. Res. Commun.* **1971**, *45*, 871.
(75) De Vries, S.; Albracht, S. P. J.; Leeuwerik, F. J. *Biochim. Biophys. Acta* **1979**, *546*, 316.
(76) Ohnishi, T.; Salerno, J. C.; Blum, H. In *Function of Quinones in Energy Conserving Systems*; Trumpower, B., Ed.; Academic Press: New York, 1982; pp 247−261.
(77) Salerno, J. C. *J. Biol. Chem.* **1984**, *259*, 2331.
(78) Salerno, J. C.; Yu, Y.; Osgood, M. P.; Kim, C. H.; King, T. E. *J. Biol. Chem.* **1989**, *264*, 15398.
(79) Migita, C. T.; Iwaizumi, M. *J. Am. Chem. Soc.* **1981**, *103*, 4378.
(80) Carter, K. R.; T'sai, A.-L.; Palmer, G. *FEBS Lett.* **1981**, *132*, 243.
(81) Walker, F. A.; Reis, D.; Balke, V. L. *J. Am. Chem. Soc.* **1984**, *106*, 6888.
(82) Walker, F. A.; Huynh, B. H.; Scheidt, W. R.; Osvath, S. R. *J. Am. Chem. Soc.* **1986**, *108*, 5288.
(83) Scheidt, W. R.; Kirner, J. F.; Hoard, J. L.; Reed, C. A. *J. Am. Chem. Soc.* **1987**, *109*, 1963.
(84) Walker, F. A. *Coord. Chem. Rev.* **1999**, *185−186*, 471.
(85) Benda, R.; Schünemann, V.; Trautwein, A. X.; Cai, S.; Polam, J. R.; Watson, C. T.; Shokhireva, T. Kh.; Walker, F. A. *J. Biol. Inorg. Chem.* **2003**, *8*, 787.
(86) Innis, D.; Soltis, S. M.; Strouse, C. E. *J. Am. Chem. Soc.* **1988**, *110*, 5644.
(87) Safo, M. K.; Gupta, G. P.; Walker, F. A.; Scheidt, W. R. *J. Am. Chem. Soc.* **1991**, *113*, 5497.
(88) Iwata, S. Personal communication.
(89) Fahnenschmidt, M.; Rau, H. K.; Bittl, R.; Haehnel, W.; Lubitz, W. *Chem. Eur. J.* **1999**, *5*, 2327.
(90) Hägerhäll, C.; Aasa, R.; von Wachenfeldt, C.; Hederstedt, L. *Biochemistry* **1992**, *31*, 7411.
(91) Hägerhäll, C.; Fridén, H.; Aasa, R.; Hederstedt, L. *Biochemistry* **1995**, *34*, 11080.
(92) von Jagow, G.; Schägger, H.; Engel, W. D.; Hachenberg, H.; Kolb, H. J. C. In *Energy Conservation in Biological Membranes*; Schäfer, G., Klingenberg, M., Eds; Springer: Berlin, 1978; p 43.
(93) Howell, N.; Robertson, D. E. *Biochemistry* **1993**, *32*, 11162.
(94) Moser, C. C.; Giangiacomo, K. M.; Matsuura, K.; de Vries, S.; Dutton, P. L. *Methods Enzymol.* **1986**, *126*, 293.
(95) Nelson, B. D.; Gellerfors, P. *Biochim. Biophys. Acta* **1974**, *357*, 358.
(96) Wilson, D. F.; Erecinska, M.; Leigh, J. S., Jr.; Koppelman, M. *Arch. Biochem. Biophys.* **1972**, *151*, 112.
(97) Dutton, P. L.; Erecinska, M.; Sato, N.; Mukai, Y.; Pring, M.; Wilson, D. F. *Biochim. Biophys. Acta* **1972**, *267*, 15.
(98) T'sai, A.-L.; Palmer, G. *Biochim. Biophys. Acta* **1982**, *681*, 484.
(99) Kramer, D. M.; Crofts, A. R. *Biochim. Biophys. Acta* **1994**, *1184*, 193.
(100) Schünemann, V.; Trautwein, A. X.; Illerhaus, J.; Haehnel, W. *Biochemistry* **1999**, *38*, 8981.
(101) Bois-Poltoratsky, R.; Eherenberg, A. *Eur. J. Biochem.* **1967**, *2*, 361.
(102) Reid, L. S.; Mauk, M. R.; Mauk, A. G. *J. Am. Chem. Soc.* **1984**, *106*, 2182.
(103) Passon, P. G.; Reed, D. W.; Hultquist, D. E. *Biochim. Biophys. Acta* **1972**, *275*, 51.
(104) Funk, W. D.; Lo, T. P.; Mauk, M. R.; Brayer, G. D.; MacGillivray, T. A.; Mauk, A. G. *Biochemistry* **1990**, *29*, 5500.
(105) Walker, F. A.; Emrick, D.; Rivera, J. E.; Hanquet, B. J.; Buttlaire, D. H. *J. Am. Chem. Soc.* **1988**, *110*, 6234.
(106) Rivera, M.; Wells, M. A.; Walker, F. A. *Biochemistry* **1994**, *33*, 2161.
(107) Rivera, M.; Barillas-Mury, C.; Christensen, K. A.; Little, J. W.; Wells, M. A.; Walker, F. A. *Biochemistry* **1992**, *31*, 12233.
(108) Rodriguez-Maranon, M. J.; Qiu, F.; Stark, R. E.; White, S. P.; Zhang, X.; Foundling, S. I.; Rodriguez, V.; Schilling, C. L., III; Bunce, R. A.; Rivera, M. *Biochemistry* **1996**, *35*, 16378.
(109) Berry, M. J.; George, S. J.; Thomson, A. J.; Santos, H.; Turner, D. L. *Biochem. J.* **1990**, *270*, 413.
(110) Costa, H. S.; Santos, H.; Turner, D. L.; Xavier, A. V. *Eur. J. Biochem.* **1992**, *208*, 427.
(111) Costa, H. S.; Santos, H.; Turner, D. L. *Eur. J. Biochem.* **1993**, *215*, 817.
(112) Kirner, J. F.; Hoard, J. L.; Reed, C. A. *Abstracts of Papers*, 175th National Meeting of the American Chemical Society, Anaheim, CA, March 13−16, 1978; American Chemical Society: Washington, DC, 1978; INOR 14.
(113) Scheidt, W. R.; Osvath, S. R.; Lee, Y. J. *J. Am. Chem. Soc.* **1987**, *109*, 1958.
(114) Collins, D. M.; Countryman, R.; Hoard, J. L. J. *Am. Chem. Soc.* **1972**, *94*, 2066.
(115) Shriver, D. F.; Atkins, P. *Inorganic Chemistry*, 3rd ed.; W. H. Freeman: New York, 1999; p 235.
(116) Scheidt, W. R.; Chipman, D. M. *J. Am. Chem. Soc.* **1986**, *108*, 1163.
(117) Shokhirev, N. V.; Walker, F. A. *J. Biol. Inorg. Chem.* **1998**, *3*, 581.
(118) Quinn, R.; Valentine, J. S.; Byrn, M. P.; Strouse, C. E. *J. Am. Chem. Soc.* **1987**, *109*, 3301.
(119) Soltis, S. M.; Strouse, C. E. *J. Am. Chem. Soc.* **1988**, *110*, 2824.
(120) Quinn, R.; Strouse, C. E.; Valentine, J. S. *Inorg. Chem.* **1983**, *22*, 3934.
(121) Walker, F. A.; Simonis, U. *J. Am. Chem. Soc.* **1991**, *113*, 8652.
(122) Shokhirev, N. V.; Shokhireva, T. Kh.; Polam, J. R.; Watson, C. T.; Raffii, K.; Simonis, U.; Walker, F. A. *J. Phys. Chem. A* **1997**, *101*, 2778.
(123) Geiger, D. K.; Lee, Y. J.; Scheidt, W. R. *J. Am. Chem. Soc.* **1984**, *106*, 6339.
(124) Safo, M. K.; Scheidt, W. R.; Gupta, G. P. *Inorg. Chem.* **1990**, *29*, 626.
(125) Safo, M. K.; Nesset, M. J. M.; Walker, F. A.; Debrunner, P. G.; Scheidt, W. R. *J. Am. Chem. Soc.* **1997**, *119*, 9438.
(126) Aasa, R.; Vänngård, *J. Magn. Reson.* **1975**, *19*, 308−315.
(127) De Vries, S.; Albracht, S. P. J. *Biochim. Biophys. Acta* **1979**, *546*, 334.
(128) Adler, A. D.; Longo, F. R.; Finarelli, J. D.; Goldmacher, J.; Assour, J.; Korsakoff, L. *J. Org. Chem.* **1967**, *32*, 476.
(129) Bobrik, M. A.; Walker, F. A. *Inorg. Chem.* **1980**, *19*, 3383−3390.
(130) The fits of magnetic Mössbauer spectra of "large g_{max}" centers are not very sensitive to the other two *g*-values, so one fit was done with those *g*-values unconstrained, while the other was done assuming the tetragonality was greater than 3.0, as was found to be the case for the $[OEPFe(4\text{-}NMe_2Py)_2]ClO_4$ complex;[87] in fact, while the tetragonality of the latter complex was found to be 3.2 (from the three *g*-values of the rhombic EPR spectrum[87]), that of the TMP analogue was taken to be 3.6, in agreement with the value found for the corresponding TPP complex.[81]
(131) Safo, M. K.; Gupta, G. P.; Watson, C. T.; Simonis, U.; Walker, F. A.; Scheidt, W. R. *J. Am. Chem. Soc.* **1992**, *114*, 7066.
(132) Cheesman, M. R.; Walker, F. A. *J. Am. Chem. Soc.* **1996**, *118*, 7373.
(133) Safo, M. K.; Walker, F. A.; Raitsimring, A. M.; Walters, W. P.; Dolata, D. P.; Debrunner, P. G.; Scheidt, W. R. *J. Am. Chem. Soc.* **1994**, *116*, 7760.
(134) La Mar, G. N.; Bold, T. J.; Satterlee, J. D. *Biochim. Biophys. Acta* **1977**, *498*, 189.
(135) Munro, O. Q.; Serth-Guzzo, J. A.; Turowska-Tyrk, I.; Mohanrao, K.; Walker, F. A.; Debrunner, P. G.; Scheidt, W. R. *J. Am. Chem. Soc.* **1999**, *121*, 11144.
(136) Higgins, T.; Safo, M. K.; Scheidt, W. R. *Inorg. Chim. Acta* **1990**, *178*, 261.
(137) Hatano, K.; Safo, M. K.; Walker, F. A.; Scheidt, W. R. *Inorg. Chem.* **1991**, *30*, 1643.
(138) Little, R. G.; Dymock, K. R.; Ibers, J. A. *J. Am. Chem. Soc.* **1975**, *97*, 4532.
(139) Quinn, R.; Nappa, M.; Valentine, J. S. *J. Am. Chem. Soc.* **1982**, *104*, 2588.
(140) Munro, O. Q.; Marques, H. M.; Debrunner, P. G.; Mohanrao, K.; Scheidt, W. R. *J. Am. Chem. Soc.* **1995**, *117*, 935.
(141) Nakamura, M.; Tajima, K.; Tada, K.; Ishizu, K.; Nakamura, N. *Inorg. Chim. Acta* **1994**, *224*, 113.
(142) Ikeue, T.; Ohgo, Y.; Saitoh, T.; Nakamura, M.; Fujii, H.; Yokoyama, M. *J. Am. Chem. Soc.* **2000**, *122*, 4068.
(143) Wolowiec, S.; Latos-Grazynski, L.; Mazzanti, M.; Marchon, J.-C. *Inorg. Chem.* **1997**, *36*, 5761.
(144) Wolowiec, S.; Latos-Grazynski, L.; Toronto, D.; Marchon, J.-C. *Inorg. Chem.* **1998**, *37*, 724.
(145) Kobayashi, H.; Maeda, Y.; Yanagawa, Y. *Bull. Chem. Soc. Jpn.* **1970**, *43*, 2342.
(146) Dolphin, D.; Sams, J. R.; Tsin, T. B.; Wong, K. L. *J. Am. Chem. Soc.* **1976**, *98*, 6970.
(147) Medhi, O. K.; Silver, J. *Inorg. Chim. Acta* **1989**, *166*, 129.
(148) Polam, J. R.; Wright, J. L.; Christensen, K. A.; Walker, F. A.; Flint, H.; Winkler, H.; Grodzicki, M.; Trautwein, A. X. *J. Am. Chem. Soc.* **1996**, *118*, 5272.
(149) Grodzicki, M.; Flint, H.; Winkler, H.; Walker, F. A.; Trautwein, A. X. *J. Phys. Chem. A* **1997**, *101*, 4202.
(150) Polam, J. R.; Shokhireva, T. Kh.; Raffii, K.; Simonis, U.; Walker, F. A. *Inorg. Chim. Acta* **1997**, *263/1−2*, 109.
(151) Shokhireva, T. Kh.; Nesset, M. J. M.; Walker, F. A. *Inorg. Chim. Acta* **1998**, *272/1−2*, 204.
(152) Nesset, M. J. M.; Shokhirev, N. V.; Enemark, P. D.; Jacobson, S. E.; Walker, F. A. *Inorg. Chem.* **1996**, *35*, 5188.

(153) Koerner, R.; Wright, J. L.; Nesset, M. J. M.; Ding, X. D.; Aubrecht, K.; Watson, R.; Barber, R. A.; Tipton, A. R.; Norvell, C. J.; Mink, L. M.; Simonis, U.; Walker, F. A. *Inorg. Chem*. **1998**, *37*, 733.
(154) Vangberg, T.; Ghosh, A. *J. Am. Chem. Soc.* **1998**, *120*, 6227.
(155) Jentzen, W.; Song, X.-Z.; Shelnutt, J. A. *J. Phys. Chem. B* **1996**, *101*, 1684.
(156) Jentzen, W.; Ma, J.-G.; Shelnutt, J. A. *Biophys. J*. **1998**, *74*, 753.
(157) Ma, J.-G.; Zhang, J.; Franco, R.; Jia, S.-L.; Moura, I.; Moura, J. J. G.; Kroneck, P. M. H.; Shelnutt, J. A. *Biochemistry* **1998**, *37*, 12431.
(158) Timkovich, R. In *The Porphyrins*; Dolphin, D., Ed.; Academic Press: New York, 1979; Vol. VII, p 241.
(159) Takano, T. *J. Mol. Biol*. **1977**, *110*, 569.
(160) Phillips, S. E. V. *J. Mol. Biol.* **1980**, *142*, 531.
(161) Medforth, C. J.; Muzzi, C. M.; Shea, K. M.; Smith, K. M.; Abraham, R. J.; Jia, S.; Shelnutt, J. A. *J. Chem. Soc., Perkin Trans. 2* **1997**, 833.
(162) Ogura, H.; Yatsunyk, L.; Medforth, C. J.; Smith, K. M.; Barkigia, K. M.; Renner, M. W.; Melamed, D.; Walker, F. A. *J. Am. Chem. Soc.* **2001**, *123*, 6564.
(163) Yatsunyk, L. A.; Carducci, M. D.; Walker, F. A. *J. Am. Chem. Soc.* **2003**, *125*, 15986.
(164) Yatsunyk, L. Ph.D. Dissertation, University of Arizona, 2003.
(165) Yatsunyk, L.; Walker, F. A. Unpublished results.
(166) Teschner, T.; Yatsunyk, L.; Schünemann, V.; Trautwein, A. X.; Carducci, M. D.; Walker, F. A. To be submitted for publication.
(167) Schünemann, V.; Trautwein, A. X.; Illerhaus, J.; Haehnel, W. *Biochemistry* **1999**, *38*, 8981.
(168) Huynh, B. H.; Lui, M. C.; Moura, J. J. G.; Moura, I.; Ljungdahl, P. O.; Münck, E.; Payne, W. J.; Peck, H. D.; DerVartanian, D. V.; LeGall, J. *J. Biol. Chem*. **1982**, *257*, 9576.
(169) Costa, C.; Moura, J. J. G.; Moura, I.; Liu, M. Y.; Peck, H. D.; LeGall, J.; Wang, Y.; Huynh, B. H. *J. Biol. Chem*. **1990**, *265*, 14382.
(170) Benda, R.; Schünemann, V.; Trautwein, A. X.; Walker, F. A. *Isr. J. Chem*. **2000**, *40*, 9.
(171) Debrunner, P. G. In *Iron Porphyrins*, Part 3; Lever, A. B. P., Gray, H. B., Eds.; VCH: Weinheim, 1989; pp 137−227.
(172) Epstein, L. M.; Straub, D. K.; Maricondi, C. *Inorg. Chem*. **1967**, *6*, 1720−1724.

CR020634J